UNIVERSITÀ DEGLI STUDI
DI NAPOLI FEDERICO II

SARATH DAS K P

Shear Strengthening of RC Columns Under Extreme Events

FRP++
Advanced structural analysis and design using composite materials

Master Dissertation
European Master Course in Advanced Structural Analysis and Design using Composite Materials

Work developed under the supervision of
Professor Marco Di Ludovico
Doctor Marta Del Zoppo

Funded by
the European Union

July of 2023

DECLARATION

Name: SARATH DAS K P

Email: sharartdas_777@yahoo.co.in **Phone number:** +39 376 163 9129

Citizen Card Number: Z0029141M

Title of the Master Thesis: SHEAR STRENGTHENING OF RC COLUMNS UNDER EXTREME EVENTS

Supervisors:

Professor Marco Di Ludovico

Doctor Marta Del Zoppo

Year of Conclusion: 2023

European Master Course in Advanced Structural Analysis and Design using Composite Materials

University of Naples Federico II, 17/07/2023

Signature:

ACKNOWLEDGEMENTS

I would like to express my deepest gratitude and appreciation to all those who have supported and guided me throughout this dissertation journey.

First and foremost, I am immensely grateful to my supervisors, Prof. Marco Di Ludovico and Dr. Marta Del Zoppo, for their invaluable expertise, unwavering support, and insightful feedback. Their guidance and mentorship have been instrumental in shaping the direction and quality of this research. I am truly grateful for their patience, encouragement, and dedication.

I am deeply grateful to Dr. Danilo D'Angela for his invaluable insight and guidance in utilizing ABAQUS, which played a crucial role in the successful completion of this study. Additionally, I would like to express my sincere gratitude to Dr. Marco Gaetani d'Aragona for providing initial insights into developing the model in ABAQUS. Furthermore, I would like to extend my heartfelt appreciation to the faculty members of the Department of Structures for Engineering and Architecture at the University of Naples Federico II for their significant contributions to my academic growth.

I am also incredibly grateful and honoured to have received guidance and knowledge from the faculties and non-teaching staff involved in the FRP++ program. Their involvement provided me with a fresh perspective and invaluable knowledge, ultimately contributing to the successful completion of this work. Their expertise and passion within their respective fields have not only inspired me but also pushed me to strive for excellence.

I would like to extend my heartfelt appreciation to my family for their unconditional love, endless encouragement, and unwavering belief in me. Their constant support and sacrifices have been a source of strength throughout this journey

I am deeply grateful to my friends and colleagues, especially to Radouan Bouallala, who have provided me with valuable insights, constructive discussions, and moral support. Their friendship and camaraderie have made this journey all the more enjoyable and memorable.

Lastly, I would like to acknowledge the participants of this study, whose involvement and cooperation were essential to the completion of this research. Without their willingness to share their experiences and perspectives, this work would not have been possible.

In conclusion, I am humbled and honoured to have had the opportunity to undertake this dissertation, and I recognize that this accomplishment would not have been possible without the support and contributions of the aforementioned individuals. Their belief in me and their willingness to invest their time and expertise have made a lasting impact on my academic and personal growth.

Thank you all from the bottom of my heart.

Rinforzo a taglio di pilastri in c.a. soggetti ad eventi estremi

RIASSUNTO

Diversi paesi in tutto il mondo sono esposti al rischio di terremoti e eventi a cascata, come tsunami o frane. Da qui la necessità di soluzioni di rinforzo in grado di migliorare la capacità delle strutture di resistere non solo all'evento sismico ma anche ai conseguenti fenomeni da esso innescati. Al giorno d'oggi la conoscenza nel campo del retrofit multirischio di asset esistenti è abbastanza limitata. Il presente studio esamina specificamente i meccanismi di collasso fragile delle colonne che possono portare alla perdita della capacità portante e, quindi, al progressivo collasso locale o globale dell'edificio. Per indagare questo problema, questo studio utilizza il software agli elementi finiti (FE) ABAQUS per modellare e analizzare il comportamento di pilastri in cemento armato (RC) soggetti a sollecitazioni laterali indotte da sisma. Vengono modellati i pilastri in due diverse configurazioni: nella condizione originale, as-built, e rinforzata con fibra di carbonio (CFRP). Il pilastro as-built è governato da un comportamento fragile con crisi a taglio prima dello snervamento dell'armatura. Il complesso comportamento del calcestruzzo viene catturato utilizzando il modello di plasticità del danneggiamento del calcestruzzo (CDP), mentre l'acciaio di armatura è modellato attraverso un legame elasto-plastico. Si assume che il sistema di confinamento in CFRP abbia un comportamento perfettamente elastico e si considera una condizione di perfetta aderenza tra l'armatura in acciaio e il calcestruzzo. Allo stesso modo, si assume un legame di perfetta aderenza tra CFRP e calcestruzzo. Il pilastro è soggetto a uno spostamento laterale monotono e ad un carico di compressione assiale costante.

La validità ed accuratezza dei risultati ottenuti attraverso il modello FE è confermata attraverso il confronto con i risultati ottenuti da prove sperimentali condotte presso il Dipartimento di Strutture per l'Ingegneria e l'Architettura. La curva forza-spostamento, i valori puntuali dello stato tensionale nell'acciaio e di deformazione nel rinforzo in CFRP sono stati utilizzati per validare il modello FE con i dati sperimentali.

I risultati ottenuti dimostrano un buon accordo con tra i risultati provenienti dalla modellazione e quelli sperimentali soprattutto in termini di curva forza-spostamento. Il modello agli elementi finiti mostra un ottimo accordo nel caso di pilastro non rinforzato e conferma che il rinforzo di pilastri in cemento armato con CFRP può trasformare la modalità di crisi da fragile a duttile.

Tuttavia, ulteriori analisi sono necessarie per raffinare il modello ed ottenere un allineamento più accurato, specie nel caso del pilastro rinforzato con CFRP.

PAROLE CHIAVE: Rinforzo a taglio, CFRP, Pilastro in CA, Plasticità edanno del calcestruzzo, ABAQUS

Shear Strengthening of RC Column Under Extreme Events

ABSTRACT

Several countries worldwide are exposed to seismic hazard and cascading events, such as tsunami or landslides. This leads to the need of strengthening solutions able to enhance the capacity of structures to withstand not only the seismic event but also the subsequent hazards. Indeed, limited knowledge is nowadays available in the field of efficient multi-risk retrofit of existing assets. The study here specifically looks at brittle failure mechanisms of columns that may lead to the loss of load bearing capacity and, hence, to the local or global progressive collapse of the building.

To investigate this issue, the study employs the finite element (FE) software ABAQUS to model reinforced concrete (RC) columns under lateral loading induced by a seismic event. Two column types are modelled: one in its original, as-built condition and the other strengthened with carbon fibre reinforced polymer (CFRP). The as-built column behaviour is governed by shear failure before the flexural yielding of longitudinal rebars. The behaviour of concrete is captured using the concrete damage plasticity (CDP) model, while the plasticity model represents the reinforcement steel. The CFRP confinement is assumed to be perfectly elastic, and a no-slip condition is considered between the steel reinforcement and concrete. Likewise, a perfect bond is assumed between the CFRP wraps and the concrete. The column is subjected to a monotonic lateral displacement and a constant axial compressive load.

The validity and accuracy of these FE models is confirmed by comparing their outputs with experimental results reported in the existing literature. Parameters such as the load-displacement curve, principal stresses in the steel, and strain in the CFRP strips are used to validate the FE model. The experimental analysis involves cyclic loading, and the hysteresis curve's envelope is used to validate the FE model's output.

The obtained results demonstrate a good agreement with the experimental analysis. The load-displacement curve exhibits a satisfactory match with the FE model's output. The FE model confirms that CFRP strengthening can transform the failure mode from brittle to ductile. However, further research is required to achieve a more accurate modelling in the case of the CFRP-strengthened columns.

KEYWORDS: Shear strengthening, CFRP, RC Column, Concrete Damage Plasticity, ABAQUS

TABLE OF CONTENTS

LIST OF FIGURES

LIST OF TABLES

LIST OF ABBREVIATIONS AND SYMBOLS

Abbreviations

CDP	Concrete Damage Plasticity
CFRP	Carbon Fibre Reinforced Polymer
C3D8R	Continuum Element - Three Dimensional with 8 nodes with Reduced integration
EBR	Externally Bonded Reinforcement
EBROG	Externally Bonded Reinforcement on Groove
FE	Finite Element
FRCC	Fibre-Reinforced Cementitious Composites
FRP	Fibre Reinforced Polymer
GFRPU	Glass Fiber Reinforced Poly Urea
NSM	Near Surface Mounted
PEEQT	Tensile Equivalent Plastic Strain
RC	Reinforced Concrete
RP	Reference point
S4R	Shell Element with Four node Reduced Integration
TRC	Textile Reinforced Concrete
T3D2	Truss- Three-Dimensional 2 node
UHPFRC	Ultra-High Performance Fiber Reinforced Concrete

Symbols

Latin Upper-case Letter

A_c	Concrete gross cross-sectional area
A_s	Total longitudinal reinforcement area
E_{cm}	Mean elastic modulus of concrete
E_f	Elastic modulus of the carbon fibre
E_s	Modulus of elasticity of steel
E_1	Longitudinal elastic modulus of laminate
E_2	Transverse in plane elastic modulus of laminate

E_3	Transverse out of plane elastic modulus of laminate
F_{max}	Peak force
G_{12}	Longitudinal shear modulus
G_{23}	Transverse shear modulus
K	Material parameter
L_s	Shear Length
S1	As-built specimen
S4	CFRP strengthened specimen

Latin Lower-case Letter

b	Width of the column
d	Displacement
d_c	Concrete damage in compression
d_t	Concrete damage in tension
f_{cm}	Ultimate compressive strength of concrete
f_{tm}	Ultimate tensile strength of concrete
f_{yl}	Yield strength of longitudinal reinforcement (Steel)
f_{yw}	Yield strength of transverse reinforcement (Steel)
h	Height of the column
$q(CM)$	Second stress invariant on the compressive meridian
$q(TM)$	Second stress invariant on the tensile meridian

Greek Letters

Υ	Normalized compressive axial load
Δ	Drift ratio
Δ_{Fmax}	Drift ratio at peak force
δ_{Fmax}	Enhanced strength
ϵ	Flow potential eccentricity
ε_c	Total compressive strain in concrete
ε_{c1}	Strain at peak stress
ε_c^{in}	Compressive inelastic strain
ε_c^{pl}	Compressive plastic strain

ε_{cu1}	Nominal ultimate strain
ε_f	Strain measured in CFRP
ε_{fu}	Ultimate strain of CFRP
ε_t	Total tensile strain in concrete
ε_t^{in}	Tensile inelastic strain
ε_t^{pl}	Tensile plastic strain
ε_{oc}^{el}	Elastic compressive strain corresponding to undamaged material
ε_{ot}^{el}	Elastic tensile strain corresponding to undamaged material
ν	Poisson's ratio
ν_{12}	In-plane Poisson's ratio
ν'	Viscosity parameter
ρ_f	FRP reinforcement ratio
ρ_l	Longitudinal steel geometric reinforcement ratio
ρ_w	Transverse steel geometric reinforcement ratio
σc	Compressive stress in concrete
σ_t	Tensile stress in concrete
Ψ	Dilation angle

THIS PAGE WAS INTENTIONALLY LEFT BLANK

1. INTRODUCTION

1.1. Introduction

During a seismic event, buildings are subjected to various types of forces, including lateral and vertical forces, which can cause significant damage and even collapse if the building is not properly designed or strengthened. One of the key elements that need to be strengthened for seismic resistance are short columns. Short columns are columns that have a low height-to-width ratio, and they are more prone to failure against shear forces than long columns. During extreme events like earthquakes or tsunami one of the major causes of the failure or collapse of existing columns is due to the shear force. This is due to old construction methods adopted combined with obsolete building codes provisions. The shear failure is a brittle failure which is not preferred due to safety reasons and to prevent complete collapse of the building.

To strengthen shear critical columns several techniques can be used. One approach is to add steel reinforcement to the column to increase its strength and ductility. Another approach is to increase the size of the column, so it can better resist the shear forces. Additionally, proper detailing of connections between the columns and the beams is essential to ensure that the building can transfer the loads safely and effectively.

Overall, strengthening shear critical columns is critical for ensuring the safety and stability of buildings. By implementing proper seismic design and strengthening techniques, the risk of building collapse can be significantly reduced, and the safety of building occupants can be greatly improved. There are several techniques that can be used to strengthen columns, depending on the specific requirements and conditions of the building. Here are some common techniques[1]:

Steel jacketing

This technique involves adding a layer of steel around the existing column to increase its strength and ductility. The jacket can be either a continuous wrap around the column or individual plates that are welded or bolted together. The steel jacketing can also help to confine the concrete core of the column,

preventing it from spalling during seismic events. To boost the column strength, various arrangements of steel jackets, plates, external ties, partial jackets, full jackets, and different steel forms have been used. The fundamental design comprises of longitudinal steel angles or channel sections that are fixed at each corner of the column and into which horizontal steel sheets are welded at strategic intervals along the column. To increase the effectiveness of the device, a small gap is left between the steel jacket and the column. Figure 1.1 shows an example of steel jacketing with and without head connections.

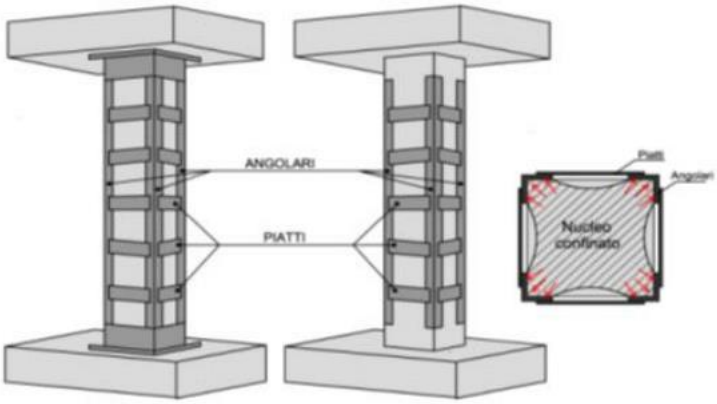

Figure 1.1: Steel jacketing with and without head connection[2]

The main advantage of this technique is that this is suitable for non-ductile and non-damaged columns. Also, this steel jacketing process results in a minor increase in column dimension, is less expensive, and speeds up construction. But the main disadvantages are the aesthetically it is not pleasing also the chances of corrosion under extreme environmental conditions and poor resistance to fire.

Concrete Jacketing: For the repair and strengthening of existing RC columns, traditional reinforced concrete jacketing has been employed extensively. The column is covered by an additional jacket made of a better concrete and an additional steel reinforcement. To improve the bond between the column and additional layers, adhesive material or anchorage bolts can be utilized. Apart from the traditional RC jacketing, Fibre Reinforced Cement Composites (FRCC) are also used for strengthening the columns. FRCC are high-strength, high-performance materials that combine a dense matrix of cementitious binder with a high-volume fraction of fine fibres, such as steel or synthetic fibres. When applied to RC columns, FRCC can significantly improve their performance under axial and lateral loads. Typical concrete jacketing configurations are shown in the figure 1.2 which provides the configuration of un-jacketed vs FRCC jacketed vs the traditional method.

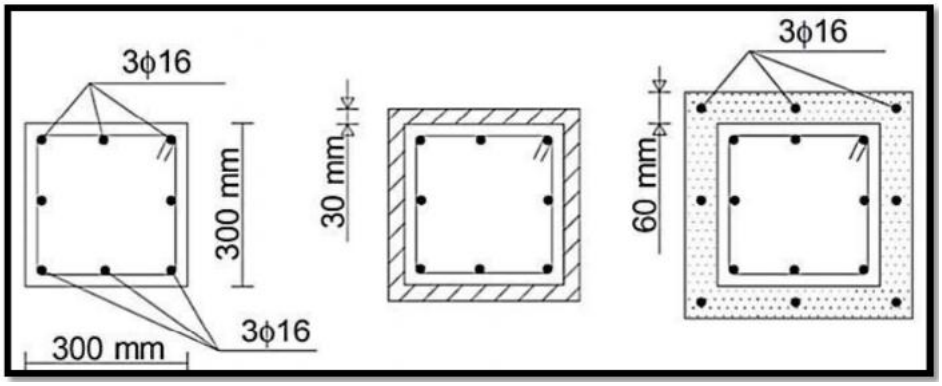

Figure 1.2: Geometry of un-jacketed, FRCC jacketed and traditional jacketed sections [3]

Depending on the type of jacket used, concrete column jacketing can restore strength, ductility, stiffness, or a combination of the aforementioned attributes. The key benefits of this approach are that it stiffens the structure and enhances the column's seismic performance in terms of axial load carrying capacity, flexural and shear strength, and ductility. Traditional reinforced concrete jackets create enlargement in column sections, add extra weight, and take longer to construct, which are the main drawbacks of this technology. These issues are partially solved by the use of FRCCs, which allows the reduction of the jacket thickness and simplify the is situ application.

Fiber-reinforced polymers (FRP): FRP materials, such as carbon or glass fibres, can be used to wrap around the column to enhance its strength and stiffness. The FRP wrapping (figure 1.3) can be applied in several layers and anchored to the column using epoxy or other adhesive materials. Carbon Fibre Reinforced Polymer (CFRP) strengthening of columns is a widely used technique for enhancing the structural performance of reinforced concrete (RC) columns. CFRP consists of high-strength carbon fibres embedded in a polymer matrix, providing excellent tensile strength and stiffness. When applied to RC columns, CFRP can increase the load-carrying capacity, ductility, and durability of the structure. The CFRP strengthening can be achieved through various methods, such as externally bonding CFRP sheets or strips to the column surface, or by wrapping CFRP fabrics or tapes around the column. The CFRP material is lightweight, corrosion-resistant, and has high strength-to-weight ratio, making it an effective choice for column strengthening. CFRP strengthening increases the flexural and shear capacity of columns, improves resistance against seismic forces, enhances crack control, and mitigates progressive collapse. It is a proven retrofitting technique that extends the service life of RC columns, allowing them to withstand higher loads and harsh environmental conditions.

Figure 1.3: Columns strengthening using FRP composites[4]

The major advantages of this method are high strength and stiffness, corrosion resistance, ease of application, light weight, improved durability of the column etc. which are explained below.

- High strength: CFRP has a very high tensile strength, which means it can withstand significant loads and stresses. This makes it an ideal material for strengthening columns that may be subjected to high seismic forces or other types of loads.
- Lightweight: CFRP is much lighter than steel or concrete, which makes it easier to handle and install. This is important where access to the columns may be limited or the building's existing structure cannot support heavy loads.
- Corrosion Resistance: CFRP materials are non-metallic and inherently corrosion-resistant. This makes them an ideal choice for strengthening columns in corrosive environments or structures prone to deterioration caused by moisture or aggressive chemicals.
- Ease of Application: CFRP strengthening is relatively straightforward and can be applied externally by bonding CFRP sheets or strips to the column surface or by wrapping CFRP fabrics or tapes around the column. This ease of application allows for efficient and cost-effective retrofitting.
- Durable: CFRP is resistant to corrosion and degradation, which means it can provide long-lasting protection to the column. It is also resistant to environmental factors such as moisture and UV light, which can damage other types of materials over time.
- Flexibility: CFRP can be easily shaped and applied to different parts of the column, including irregular or complex shapes. This flexibility allows for customized solutions that can be tailored to the specific needs of the building.

- Cost-effective: Compared to other types of strengthening materials, such as steel or concrete, CFRP can be a more cost-effective solution. It requires less labour and time for installation, and it can often be installed without disrupting the building's occupants or operations.

1.2. Motivation

Several countries worldwide are exposed to seismic hazard and cascading events, such as tsunami, landslides, earthquakes etc. This leads to the need of strengthening solutions able to enhance the capacity of structures to withstand not only the seismic event but also the subsequent hazards. The study will specifically look at brittle failure mechanisms of columns that may lead to the loss of load bearing capacity and, hence, to the local or global progressive collapse of the building. Shear strengthening with CFRP is becoming a popular method of strengthening of columns which also need more input to develop a design equation for the same and this study will give a stepping stone to the path. The shear strengthening of reinforced concrete (RC) columns using CFRP is a compelling topic for several reasons:

- Importance of Shear Strength: As many existing structures built with old code lacks the stirrups to resist to lateral displacement which in turn causes a shear brittle failure, it is necessary to restrict the collapse of buildings. Shear failure is a critical mode of failure in RC columns, especially in earthquake-prone regions. Enhancing the shear strength of columns is essential for ensuring the structural integrity and safety of buildings and infrastructure.

- Increasing Demand for Retrofitting Techniques: With aging infrastructure and stricter seismic design codes, there is a growing need for effective retrofitting techniques. Shear strengthening using CFRP offers a promising solution to enhance the performance of existing RC columns, extending their service life and improving their resistance to seismic forces.

- Advancements in CFRP Technology: CFRP materials have shown significant potential in enhancing the shear strength of RC columns. Recent advancements in CFRP technology, such as improved bonding agents and innovative reinforcement layouts, have further expanded their effectiveness as a retrofitting solution.

- Sustainability and Durability Considerations: The use of CFRP for shear strengthening can contribute to sustainability goals by extending the life cycle of existing structures, reducing the need for resource-intensive construction of new infrastructure. Additionally, CFRP's corrosion resistance can enhance the long-term durability of the columns, reducing maintenance requirements.

- Research Gap and Contribution: While there is existing research on the shear strengthening of RC columns using CFRP, there may still be gaps in knowledge and understanding. A study focusing on this topic can contribute to the field by investigating specific aspects, such as the effects of different strengthening techniques, optimization of CFRP layouts, long-term performance, and the behaviour of strengthened columns under various loading conditions. A reliable model is necessary to achieve these goals.

- Practical Relevance and Engineering Applications: The findings of the study can have practical implications for engineers involved in the design and retrofitting of RC structures. The research outcomes can provide valuable insights into the design guidelines, construction practices, and cost-effectiveness of shear strengthening using CFRP for RC columns.

By choosing to focus on the shear strengthening of RC columns using CFRP in, the opportunity to contribute to the body of knowledge in this field, address existing research gaps, and make a significant impact on the advancement of structural engineering practices related to the retrofitting of RC structures.

1.3. Problem Statement

Recent seismic events worldwide clearly demonstrated that the brittle failures due to lack of shear reinforcement in columns are the most frequent mechanism of collapse of existing buildings [5]; the use of FRP as strengthening solution to fill the shear capacity gap of such member is continuously growing. There are experimental studies conducted for FRP strengthened columns under horizontal actions. But these experimental studies are costly, time consuming, and need skilled labour. The study here aims to contribute to overcome the practical difficulties of experimental investigation and to develop a numerical model for both the as-built specimen and the CFRP strengthened specimen and compare it with the

experimental result obtained from the study conducted by Del Zeppo et.al. [5] and validate the numerical model.

The aforementioned study [5] serves as an input to the FE model. The input data includes the specimen geometry, material properties and loading protocols. Then the numerical model for the as-built specimen and CFRP strengthened specimen is developed by starting with the geometry. The material properties for concrete, steel and CFRP was implemented. For concrete, the Concrete Damage Plasticity model was adopted while defining the material properties, to accurately capture the degradation of the concrete. For steel an elastic- plastic behaviour was modelled. Whereas in the case of CFRP only elastic regime was modelled. The whole model was meshed using appropriate element type. Apart from the axial load, the horizontal displacement was implemented in the model. The experimental study was done with cyclic loading, whereas the FE model defined here uses monotonic loading condition for simplicity, with the same rate at which the lateral displacement was provided in that of the experimental one. Once all the loading and boundary conditions were defined, various interactions were defined. The interaction between CFRP and concrete was defined as perfectly bonded. The results from the FE model taken includes the load displacement curve, the principal stress in steel, the crack pattern and the strain in the CFRP wrapping. The results from the numerical model were then validated using the experimental study.

1.4. Objectives

The main objective of this work is to develop a numerical model and study the shear strengthening of RC columns under extreme events using CFRP. The major objectives are as follows:

1. To develop a numerical model for an RC column undergoing a quasi-static monotonic loading.
2. To investigate the effect of CFRP wrapping for shear strengthening of RC Columns
3. To compare and validate the developed numerical model with the experimental results.

The research conducted in this study and the objectives achieved will contribute in the formulation of design equations for columns strengthened with FRP under axial loading along with the extreme events.

1.5. Structure of the Dissertation

The following methodology was used to complete this study.

1. Previous investigations and studies were collected and reviewed to construct an optimal model for the analysis.
2. A numerical model was developed to carry out the analysis for both the as-built specimen and CFRP strengthened configuration as per the experimental data[5].
3. The results obtained were analysed and validated with the experimental values.
4. The effect of CFRP strengthening was discussed.

2. LITERATURE REVIEW

2.1. Introduction

The increased seismic activities faced by the world is demanding not only for improved design of structures, but also questions the integrity of the existing structures due to the gaps existed in the old codes which couldn't foresee the extreme events like landslide, earthquakes, tsunamis etc. And most of them which are built when the design was not focused to face seismic events are demanding strengthening. And this strengthening necessitates the safety and functionality of these existing structures. Many elements of a structure get affected due to seismic events and one of the major issues is the lack of shear strengthening in short columns. Most of the existing structures have been designed according to old codes and lack of stirrups in these short columns are causing a brittle failure of these columns. So, the major focus of this session is to strengthen the short columns using appropriate methods.

There are many strengthening techniques for the existing structures like steel jacketing, using FRCC, FRP confinement etc. Strengthening with steel is good, but the chances of corrosion and increase of weight makes it difficult for being an ideal candidate for shear strengthening. The major focus of the study is strengthening using FRP materials.

Even Though strengthening of short columns with FRP has provided good results in the past, the need of having a numerical model is inevitable these days. So that this will help to reduce the cost of experiments, can save a lot of time and will give a semi empirical result. So, this literature review has been divided into 3 parts which can be focused on the following areas:

1. Strengthening techniques of existing RC Columns
2. Experimental validation under extreme events of cascading
3. Numerical models to study the effect of FRP strengthening.

Several research studies have investigated the use of CFRP for shear strengthening of columns, with most studies showing positive results in terms of improved shear capacity and ductility. Here are some salient results from recent research:

2.2. Strengthening Techniques of RC Columns

As mentioned earlier there are several strengthening techniques of columns like steel jacketing, concrete jacketing, FRP confinement, grouting etc. Out of these the FRP wins marginally on different aspects and the main focus of the topic here is to investigate the improvement in shear strength of by FRP confinement.

In a study conducted by Del Zoppo et.al., [5] , researchers studied the column shear failures in RC buildings severely damaged after the L'Aquila earthquake. The experimental study was carried out on seven short columns which were governed by shear failure under compressive axial load and load reversal. And the studies were conducted on two classes of concrete. The one with the poor quality of concrete produced an increase in 56% to 67% the original shear capacity of the short RC columns by the introduction of the CFRP confinement with axial rigidity ($E_f\rho_f$) lower or equal to 0.31 GPa. Investigation for medium quality concrete strengthened with two plies of concrete resulted in plastic deformation with ultimate drift ratio greater than 8.5%. And this paper is also the reference for validating the numerical model developed in this study.

The research by A.J. Naji et.al [1] found that CFRP and GFRP has many advantages compared to other traditional techniques. Contrary to steel plates and concrete jackets, CFRP sheets offer a high strength to weight ratio and very high resistance to corrosion and chemical attacks, making them ideal for constructions exposed to hostile conditions. Whereas RC columns can be strengthened using excellent composites made of glass fibre reinforced polymers (GFRPs). They have demonstrated good performance and durability, and due to their low weight and small increase in member dimensions, they are frequently used in the construction industry. Additionally, the GFRP strengthening approach saves time.

A. Kargan et.al.[6] investigated about the shear failure involved in structures that occur in short columns. The study was done both experimental and numerically. The investigation pointed out that strengthening using FRP with full wrapping changed the behaviour and failure mode of the short columns from shear to flexural. They also studied the hybrid technique of using FRP along with EBR which also resulted in delayed deboning and rupture which showed promise in improving performance under cyclic loading. The performance was measured in terms of fracture at delayed drift. The load carrying capacity with

strengthened specimen indicated an increase from 128% to 159% which showed a positive response in strengthening with FRP.

Hosseini S et.al [7] has argued that on resisting the plastic hinge formation on short columns during low drift ratios can cause high risk during earthquakes. The study conducted included four RC short columns strengthened with FRP and one as-built specimen. The strengthening was done as externally bonded reinforcement on grooves (EBROG) and externally bonded reinforcement (EBR), the number of longitudinal carbon fibre reinforced polymer (CFRP) layers (0–2), and the partial usage of longitudinal FRP sheets were all some of the test parameters. According to the results, shear-flexural retrofitting of short columns using longitudinal CFRP sheets applied via the EBROG method along with an adequate number of confined CFRP wraps increased the load-carrying capacity, ductility, and dissipated energy by up to 83%, 168%, and 1,200%, respectively, in comparison to those obtained for the unstrengthened specimen. At the same time CFRP confinement for shear strengthening resulted an increase in load carrying capacity by 29% and ductility by 26% and around 137% of dissipated energy was increased. Which all pointed to the enhancement of performance of CFRP confined columns causing the chance of failure by flexural rather than shear.

2.3. Experimental Validation Under Extreme Events

Existing RC columns with borderline flexure and shear behaviour were studied in 2018 by Del Zoppo et.al.[8] , with both medium-quality concrete and strong FRP with local jacketing and poor-quality concrete with moderate FRP strengthening. In addition to the FRP jacketing, the Fiber Reinforced Cementitious Composite (FRCC) jacketing's efficiency for seismically fortifying columns with severely degraded concrete covers or columns that have already sustained earthquake damage was assessed in this investigation. According to the study, when comparing columns made of poor and medium quality concrete, it was discovered that the local jacketing made of CFRP is more effective in the case of poor-quality concrete while the jacketing made of FRCC appears to be a sound repair method and a good substitute for the FRP jacketing in the same situation. Six full-scale RC columns were put through cyclic loading testing; one served as a reference specimen, four had their potential plastic hinge region reinforced with carbon fibre reinforced plastic (CFRP), and one had FRCC entirely jacketed. In the possible plastic hinge region, CFRP-jacketed specimens had a flexural behaviour that avoided the shear interaction mechanism and significantly improved in ductility compared to the control specimen. When dealing with concrete columns

of inferior quality, CFRP jacketing was more useful. The initial lateral stiffness and post-peak strength degradation of the columns were controlled by the axial rigidity of the composite system.

Song J et.al [9] studied shear strengthened RC Columns retrofitted by glass fibre reinforced polyurea (GFRPU). Four strengthened specimens along with an unstrenghtened specimen were tested to evaluate the parameters of the GFRPU against axial compressive load and cyclic loading. The strengthening was done partially and fully and the structural strengthening effect of GFRPU was analysed. The strengthening resulted in an increase in the shear resistance capacity by 8-9%. The specimen with full confinement showed a better load carrying capacity than that of the one with partial strengthening. Thus, the area of confinement also proved to be crucial for restricting the formation of plastic hinge zone. In comparison to the specimen strengthened with polyurea, the specimen strengthened with GFRPU showed greater strength and energy dissipation capacity.

K Gajdosova et.al. [10] tested CFRP strengthened slender reinforced concrete columns. Two approaches were used for strengthening of the columns. The first one was the well-known approach of CFRP sheet jacketing and the second a relatively new one with near surface mounted (NSM) CFRP strips. A total eight full scale model was tested. The test resulted in that the confinement was the most effective in the case of compressive stress for short columns. And the NSM proved to be most effective in the case of tensile behaviour. Longitudinal NSM CFRP strips exhibited more effective against flexure. Though confined columns showed better performance, the best ductile post peak behaviour occurred for the columns with longitudinal NSM CFRP strip. Even with the quasi-ductile behaviour the failure mode of columns was by crushing and spalling of concrete. But the size of crack was limited in the case of the strengthened columns.

2.4. Numerical Models for Shear Strengthening of RC Columns

Li Y et.al[11] investigated the seismic performance of textile reinforced concrete (TRC). It was done on a RC Column and the investigation was done in FE (Finite Element) software ABAQUS. The TRC strengthened columns were able to restrict the development of crack. While analysis it exhibited that with increasing axial compression ratio, the reinforced columns' bearing capacity and stiffness degradation rate increased, but the displacement ductility coefficient and energy dissipation capacity showed the reverse trend. The ductility, deformation capacity, and cumulative energy dissipation capacity of the

strengthened columns rose as the shear span ratio increased, but the columns' bearing capacity declined. The maximum load of reinforced columns grew along with the grade of concrete strength. The displacement ductility coefficient and accumulated energy dissipation capacity increased with increasing concrete strength grade when the concrete grade was within C40.

F Dhanesh et.al [12]investigated about the FE study of shear strengthening of RC beam-column connection using GFRP. The model was validated with a previously tested model done experimentally. The experimental program compared the hysteresis curves of models with and without strengthening. But in the FE model a monotonic loading protocol was applied. And the load-displacement curve obtained was compared with the downward loading response of the envelope curves of the experimental tests. The material property for the concrete was implemented by the well-known Concrete Damage Plasticity model (CDP). For steel reinforcement the study was done using the truss element T3D2. And for the GFRP a four-node shell element (S4R) was used for the analysis. It was considered a full bond between GFRP and the concrete model for simplicity. Though the study represented a better behaviour of the strengthened specimen compared to the as-built, the failure mode was not changed completely from shear to ductile.

The research conducted by Altaee M et.al [13] regarding the damage plasticity model for concrete members subjected to high strain-rate analysed the influence of several parameters like dilation angle, eccentricity parameter and tensile behaviour of the concrete. The results pointed that the dilation angle between 45° to 50° provided better correlation with the experimental results. The eccentricity parameter was tested with a range between 0.1 to 0.2 and the displacement -time history provided a better accuracy when this value was in between 0.10 and 0.15. The tensile behaviour consisted bilinear stress-strain, tri-linear stress-strain and stress-crack opening displacement models, which resulted in tri-linear being the best among the three for tensile softening.

THIS PAGE WAS INTENTIONALLY LEFT BLANK

3. EXPERIMENTAL INPUT DATA AND RESULTS

3.1. Introduction

The main objective of this chapter is to present the details of the experiment data and results which gave input for the FE modelling and validation. The data input includes the geometrical details used in modelling the specimens in ABAQUS, the loading protocol and the discussion of the relevant results which is used to validate the FE model.

3.2. Experimental Details

The numerical model presented in this study was developed based on the experimental investigations carried out by Del Zoppo et al. [5]. The study was conducted in response to the L'Aquila earthquake that occurred on April 6, 2009, with a magnitude of 6.3, resulting in the severe damage of numerous reinforced concrete (RC) structures. The comprehensive analysis performed by the authors; it was observed that approximately 20% of the structures experienced brittle failure due to shear forces. The authors identified several factors contributing to these failures, including the poor quality of concrete, insufficient shear reinforcements, and the absence of longitudinal reinforcement in one direction, among others. These structures were constructed using outdated design codes that were incapable of anticipating such extreme events, ultimately leading to the eventual collapse of the buildings.

The purpose of selecting these structures was to analyse and investigate the occurrence of shear failure and propose a viable solution to prevent such failure modes by enhancing their shear capacity through the use of CFRP (Carbon Fiber Reinforced Polymer) wrappings. The authors replicated the outdated design codes and designed a total of seven short columns for their study. Among these columns, two were kept in their original as-built condition without any strengthening, while the remaining five columns were strengthened using CFRP materials.

The two as-built specimens represented different qualities of concrete, with one column made of low-quality concrete and the other column made of medium-quality concrete. Similarly, out of the five CFRP-strengthened columns, three represented low-quality concrete, and the remaining two represented

medium-quality concrete. This setup allowed the authors to compare the performance of the original as-built columns with those that were strengthened using CFRP, taking into consideration different concrete qualities.

The scope of the study here only encompasses the two specimen- one the as-built specimen with low quality concrete (Specimen S1 as per the paper) and a low-quality concrete CFRP strengthened specimen (S4). The numerical model developed was based on these two specimens, so the study only investigates and present data regarding these specimens.

The numerical model developed in this study focused on two short columns: one as-built specimen and the other a CFRP-strengthened specimen. Both columns had a square cross-section and were susceptible to shear failure. The specimen chosen for the numerical analysis was the one with poor-quality concrete. These specimens were subjected to a horizontal cyclic quasi-static displacement while being loaded with an axial load ratio of 0.1. The design of the experimental column was based on the shear failure observed in buildings during the L'Aquila earthquake that occurred on April 6, 2009, with a magnitude of 6.3. The vulnerability of the columns to shear failure was attributed to the absence of sufficient transverse reinforcement in the existing columns. In the following section, a detailed description of the specimen geometries, mechanical properties, and the load protocol used in the study will be provided.

3.2.1. Specimen Geometry and Mechanical Properties

The short columns in this study were intentionally designed to be excessively strong in flexure, resulting in a brittle failure mode. Both the as-built specimen (S_1) and the CFRP-strengthened specimen (S_4) had identical dimensions. They featured a square cross-section measuring 300 × 300 mm^2 and were reinforced with ten deformed rebars of 22 mm diameter rebars (resulting in a longitudinal geometric reinforcement ratio, $\rho_l = A_s/bh = 4.2\%$ with A_s being the total longitudinal steel reinforcement area and b×h the cross-sectional dimension of the column)

For both specimens, the concrete cover thickness was 20 mm. The transverse reinforcement in the columns consisted of 8 mm diameter ties spaced at 300 mm intervals (resulting in a transverse geometric reinforcement ratio, ρ_w, of 0.11%). The ties were equipped with hooked ends. In the experimental setup,

a reduced spacing of transverse reinforcement was adopted in the load application zone to prevent localized damage.

The specimen were columns with a foundation block. The columns were with a height of 1250 mm and the foundation block were having a dimension of 1200 × 1200 × 600 mm^3. The lateral load was applied at a distance of 900 mm from the foundation block in order to reproduce the behaviour of the short columns. That is the L_s/h ratio was 3, where L_s was the shear length (900 mm) and h was the height of the column.

The summary of the material properties is shown in the table 3.1. The as-built specimen had a low concrete strength of 14.3 MPa and that for the strengthened specimen, S4 had a concrete strength of 14 MPa. The two specimens were selected due to the fact that these two had a comparable class of strength and the FE analysis results will be a lot easier to compare. And also, the specimen S4 was chosen due to the fact that the failure was of a quasi-ductile failure.

Table 3.1: Material Properties

Specimen	f_{cm} (MPa)	f_{yl} (MPa)	f_{yw} (MPa)	No. of plies
S1	14.3	531	525	-
S4	14			1

The S4 specimen underwent reinforcement using CFRP (Carbon Fiber Reinforced Polymer) strips. These strips, measuring 100 mm in width, were positioned at intervals of 165 mm along the entire height of the column, as depicted in figure 3.1. To prevent premature fibre rupture, the corners of the columns were rounded with a radius of 20 mm. However, in the Finite Element (FE) model, this step was not taken into account due to the significant impact it would have on the mesh size. Consequently, comparing the actual construction with the CFRP-strengthened version in the FE model would not yield reasonable results. Additionally, the experimental setup involved a strip overlap of 250 mm for each layer, which was disregarded in the FE model as a perfect bond between the concrete and CFRP strips was assumed.

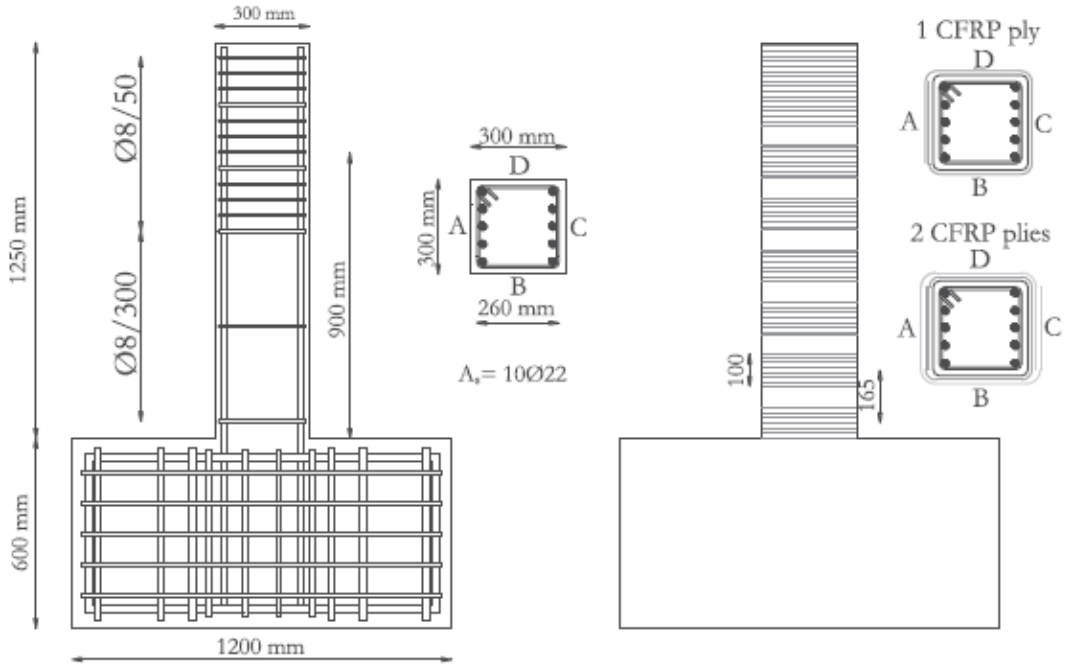

a) As-built specimen – S1 b) CFRP Strengthened Specimen- S4

Figure 3.1: Specimen geometry

There were different CFRP used in the study. The one this study uses has a unit weight of 600 g/m^2 and an ultimate strain ε_{fu} = 1.9% and the elastic modulus of dry fibres E_f= 252 GPa was considered for the analysis.

3.2.2. Test- setup and loading protocol

The specimens in this study were subjected to a constant compressive axial load and cyclic lateral displacement. However, in the Finite Element (FE) model used for analysis, a monotonic lateral displacement was applied instead of cyclic loading. This decision was made because simulating cyclic displacement in the FE model would be computationally intensive and time-consuming. The axial load remained the same as in the experimental setup.

For applying the lateral load, an electrohydraulic actuator was used at a distance of 900 mm from the base of the column (shear length), as shown in figure 3.2a. The actuator had a stroke of ± 250 mm and load extremities of + 500 kN and -300 kN, respectively.

The specimens were subjected to a normalized compressive axial load, represented by $\Upsilon = N/A_c f_{cm}$, where N is the compressive axial load, A_c is the concrete gross cross-sectional area, and f_{cm} is the mean cylindrical concrete strength. The normalized compressive axial load value was set to 0.1.

In terms of lateral cyclic loading, drift control was employed using the parameter $\Delta = d/L_s$, where d is the horizontal applied displacement, and L_s is the shear length. The testing procedure involved initial four cycles with a rate of 0.2 mm/s, followed by the next five cycles with a rate of 1.0 mm/s, and finally, the last cycles were conducted with a rate of 2.0 mm/s for the lateral displacement, as shown in figure 3.2b. To monitor the axial strain in the external reinforcement (CFRP strips), strain gauges were placed at the mid-span of each CFRP strip in all the specimens.

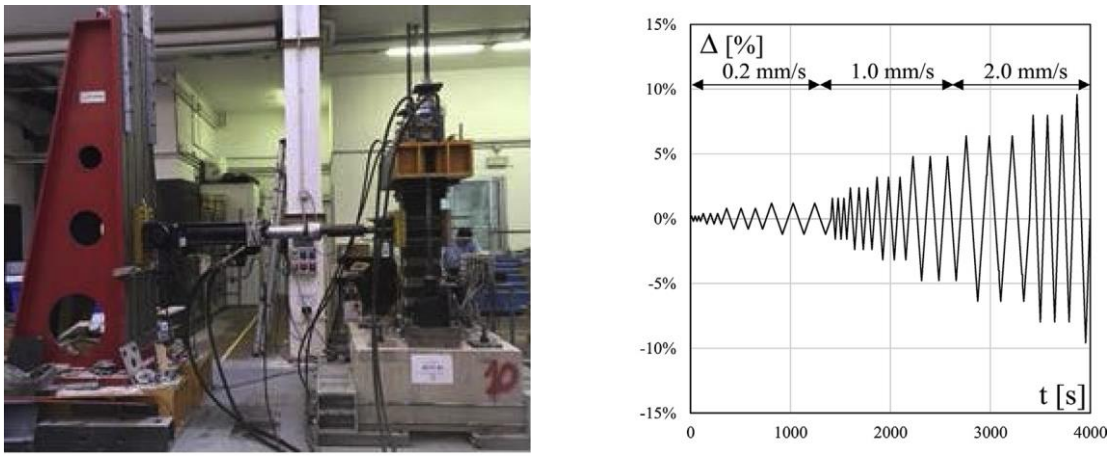

a) Test setup b) Loading protocol

Figure 3.2: Load Application[5]

3.3. Experimental Results

The experimental results presented in this analysis include relevant and comparable data from specimens S1 and S4, as mentioned previously. The focus is primarily on two aspects:

1. Lateral Load-Drift Relation: This refers to the relationship between the applied lateral load and the resulting lateral drift (displacement) of the columns. The experimental data provides

information on how the columns responded to the cyclic lateral loading in terms of their lateral displacement behaviour.

2. Strain Analysis in CFRP: This involves analysing the strain (deformation) experienced by the CFRP strips used for external reinforcement. The experimental results include measurements of the strain at different locations along the CFRP strips, allowing for an assessment of their performance and effectiveness in strengthening the columns.

The experimental results and the predictions of the FE model may be compared using these particular data, allowing for a greater comprehension of the behaviour of the reinforced columns and the precision of the model's simulations. In addition to the data described above, the strength of the steel reinforcement and the location of the crack are examined to understand the shear failure occurrence.

3.3.1. Lateral load-drift relation

Figure 3.3 illustrates the experimental load-drift relation, which shows the hysteresis curve resulting from the cyclic lateral displacement. The envelope of this hysteresis curve is particularly important for analysing the Finite Element (FE) model since the model is subjected to a monotonic loading protocol. By comparing the hysteresis curves of both the as-built and CFRP-strengthened specimens, the percentage increase in strength due to the CFRP reinforcement can be determined and is presented in table 3.2.

The as-built specimen exhibited a brittle failure primarily governed by shear, occurring before flexural yielding. Diagonal cracks developed throughout the entire shear length of the column at sides B and D, where the longitudinal reinforcement was absent. Following the peak strength, there was a sudden drop in lateral strength for the as-built specimen. The peak force was achieved at a drift ratio of 1.6% (equivalent to 14.4 mm of lateral displacement), with a peak strength of +159.6 kN (-151.8 kN).

On the other hand, the CFRP-strengthened specimen (S4) exhibited a quasi-ductile behaviour, with flexural yielding occurring before a sudden drop in lateral capacity due to CFRP rupture. In the FE model, the failure of the CFRP strip is neglected for two reasons: the lack of properties and the aim for simplicity in modelling. The use of an external reinforcement ratio of 0.4% transformed the failure mode of the specimen from brittle to quasi-ductile behaviour. The recorded peak force was approximately 286 kN,

corresponding to a strength enhancement of around 80-89% (δ_{Fmax}), at a drift ratio of 2.4% (equivalent to 21.6 mm of lateral displacement).

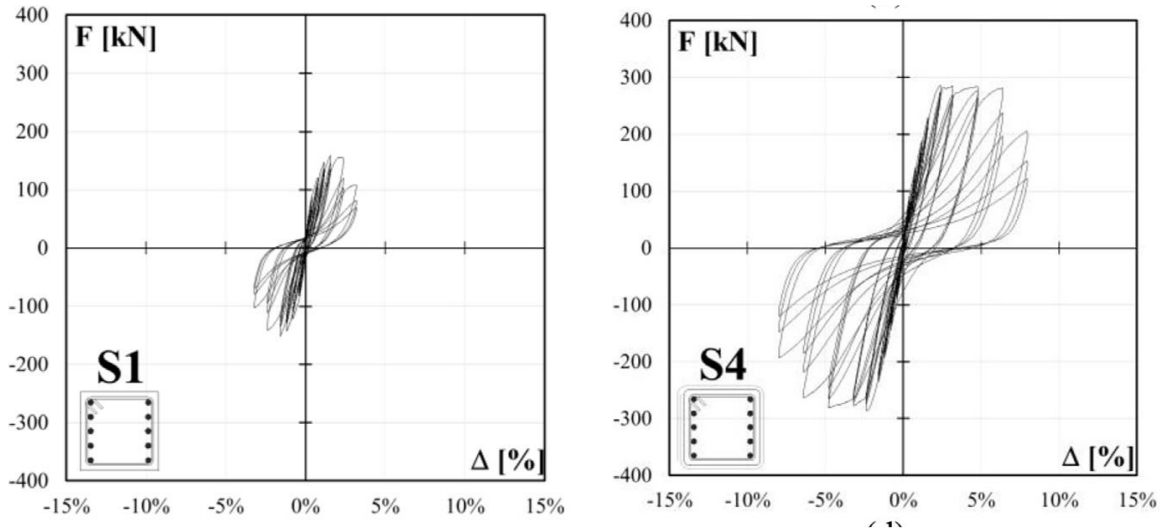

a) As- built specimen b) CFRP strengthened specimen

Figure 3.3: Lateral load-drift relationship[5]

Table 3.2: Experimental outcome[5]

Test Specimen	F_{max} (kN)	Δ_{Fmax} (%)	δ_{Fmax} (%)	Displacement (mm)	Failure mode
S1	+159.6	+1.6	-	+14.4	Shear
	-151.8	-1.6	-	-14.4	
S4	+286.7	+2.4	+80	+21.6	Flexure-shear
	-286.5	-2.4	+89	-21.6	

3.3.2. Strain analysis in CFRP

The experimental model also examines the effective strain placed on the CFRP as a result of the combined effects of shear and lateral dilatation. Utilizing strain gauges, the first four CFRP strips from the base of the columns were measured for CFRP strains at the mid-span and mid-height of each side.

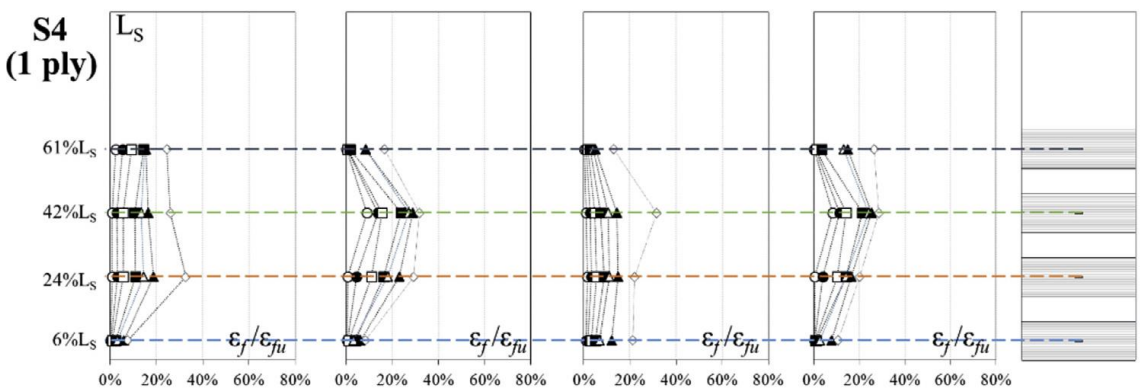

Figure 3.4: CFRP strain distribution along the column height [5]

The ratio of the CFRP experimental strain, ε_f and the ultimate CFRP strain (ε_{fu} = 1.9 %) is presented in the figure 3.4 for each side. From analysing the strain behaviour in the CFRP, it exhibits a maximum strain of around 30 % in the third strip in side B for a drift of 4.8%. The strain behaviour in numerical model is also analysed for the same drift ratio. Details of this comparison will be elaborated in chapter 4.

4. FINITE ELEMENT MODEL

4.1. Introduction

The main objective of this chapter is to present the details of the FE modelling and the discuss about the numerical model developed using ABAQUS and explain the inputs used for the analysis. For both the as-built and CFRP strengthened specimens, the modelling detail comprises the specifics of the geometry, material properties, loading protocol, and interactions developed in ABAQUS.

4.2. Specimen Geometry

As explained previously the parameters used here are from the experimental tests by Del Zoppo et.al [5]. As per the experimental program the columns were designed to fail under shear rather than flexure. Both as built and CFRP strengthened specimens have the same geometrical properties and reinforcements. The short columns had a square cross section 300× 300 mm^2 reinforced with ten 22 mm diameter deformed rebars (longitudinal geometric reinforcement ration, $\rho_l = A_s/b.h = 4.2\%$ with A_s total area of longitudinal reinforcement and b, h being the cross section dimensions). Only the loading direction received longitudinal reinforcement; there was no reinforcement in the secondary direction. Each specimen has a 20 mm thick concrete cover. Steel ties with an 8 mm diameter, 300 mm spacing, and hooked ends were used as the transverse reinforcement (transverse geometrical reinforcement ratio, $\rho_w = 0.11\%$). In order to prevent localized damage, a smaller gap has been employed in the load application zone. The cantilever specimens were created from a foundation block and a column, with the foundation block's dimensions being 1200×1200×600 mm^3 and the column's height being 1250 mm.

In the ABAQUS software, the column was divided into three parts for simulation purposes. The concrete column along with the foundation block was modelled as a 3D deformable solid, as depicted in figure 4.1. This solid model allows for the representation of the behaviour and deformation of the concrete

material. The solid model was partitioned for two reasons, one for the compatibility of mesh and the second one is for specifying the location of shear length so as to apply the lateral displacement.

For the steel reinforcement, both the transverse and longitudinal reinforcement, a deformable wire model using truss elements was employed. Truss elements are suitable for representing the steel reinforcement and are compatible with the concrete damage plasticity model (CPD) utilized in the analysis. The use of truss elements also enables the assumption of a no-slip condition between the concrete and the steel reinforcement. This configuration aligns with the actual use of deformed bars as reinforcement and contributes to the simplicity of the model.

The CFRP (Carbon Fiber Reinforced Polymer) confinement was modelled using shell elements. Shell elements are well-suited for representing thin structural components, such as the CFRP confinement in this case. The section properties of the CFRP confinement were defined according to conventional shell element specifications.

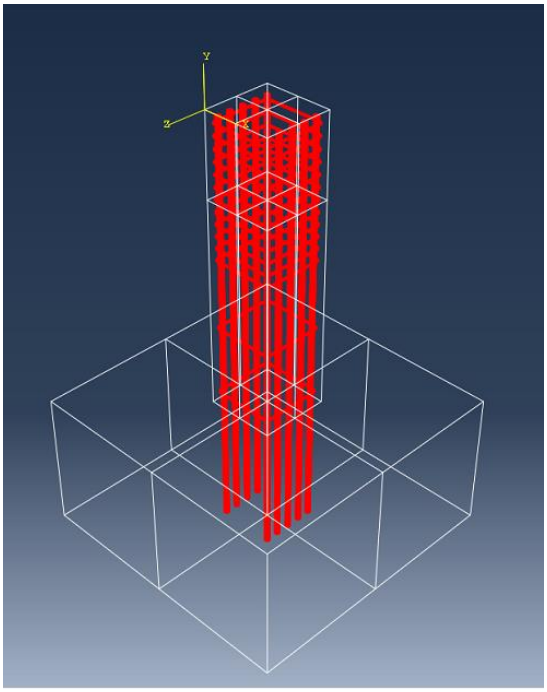

a) Wire-frame model of S1

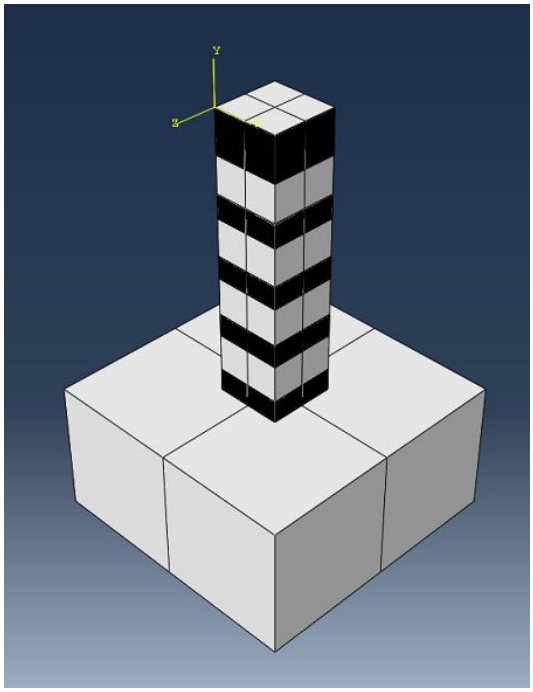

b) Shaded model of S4

Figure 4.1: RC column with the reinforcements

By employing these different modelling elements, including 3D deformable solid for concrete, truss elements for steel reinforcement, and shell elements for CFRP confinement, a comprehensive representation of the column's structural components and their interactions is achieved in the Abaqus model.

4.3. Material Properties

To obtain reasonable and accurate results in Finite Element Analysis (FEA) simulations, it is crucial to utilize appropriate material models. In the case of analysing concrete behaviour in Abaqus, the software provides a well-defined model called Concrete Damage Plasticity [14],[15]. This model takes into account the nonlinear behaviour of concrete, including its ability to undergo damage and plastic deformation. By using the Concrete Damage Plasticity model, the FEA analysis can accurately capture the response of concrete under various loading conditions.

For modelling the steel reinforcement, a plasticity model is typically employed. The plasticity model considers the nonlinear stress-strain behaviour of steel, including its ability to undergo plastic deformation. This allows for an accurate representation of the steel reinforcement's behaviour in the FEA analysis.
In the case of CFRP (Carbon Fiber Reinforced Polymer), only the elastic properties are considered in the modelling. This means that the CFRP material is assumed to behave linearly within its elastic range and does not exhibit plastic deformation or damage. While this simplification may not capture the full behaviour of CFRP, it is a common approach in FEA analysis where the focus is primarily on the overall response and load-carrying capacity of the structure.

By employing these appropriate material models, such as Concrete Damage Plasticity for concrete, plasticity models for steel, and elastic properties for CFRP, the FEA analysis conducted in Abaqus can provide reasonable and accurate results for studying the structural behaviour of the column.

4.3.1. Concrete

Concrete, being a composite material, consists primarily of cement, fine and coarse aggregate, and water. Due to the unique properties of its various components, concrete requires a constitutive model that can

accurately capture its nonlinear behaviour during analysis. In Abaqus, a Concrete Damaged Plasticity (CDP) model has been developed [14], [15] specifically for simulating concrete behaviour.

The CDP model incorporates an internal variable-formulation of plasticity theory, allowing for the representation of both compressive crushing and tensile cracking in concrete. This makes the model suitable for analysing concrete under cyclic loading conditions, as well as monotonic loading. By considering both compressive and tensile behaviours, the CDP model provides a comprehensive representation of concrete's response to various loading scenarios.

When inputting material properties for the CDP model, it is important to exercise caution to ensure reasonable results. While complete experimental material properties may not always be available, an analytical model based on Eurocode-2 [16] and documentation provided by Abaqus [17] can be utilized. These references provide guidelines and recommendations for determining the material properties of concrete, enabling a reliable comparison between experimental and analytical models.

By employing the CDP model and carefully selecting appropriate material properties, the Abaqus software facilitates accurate analysis of concrete structures, considering the complex behaviour exhibited by this material. Along with the damage plasticity model, the elastic behaviour needs to be modelled in ABAQUS. For that purpose, Elastic modulus and the Poisson's ratio are used. While designing the CDP model totally 5 plasticity parameters are used. The dilation angle (ψ), the ratio of initial equiaxial compressive yield stress to initial uniaxial compressive yield stress (f_{b0}/f_{c0}), the flow potential eccentricity (ϵ), viscosity parameter (ν'), material parameter K (defined as the ratio of the second stress invariant on the tensile meridian, q(TM), to that on the compressive meridian, q(CM)[17].

Table 4.1: Concrete damage plasticity input parameters

Dilation Angle (ψ)	ϵ	f_{b0}/f_{c0}	K	ν'
30-55	0.1	1.16	0.67	0-0.01

The values in table 4.1 are reviewed from literatures[17]. The dilation angle is a crucial parameter that affects the ductility and behaviour of the entire model. As the dilation angle increases, the system

becomes more flexible. This increase in flexibility is associated with higher plastic strain and confining pressure in practical applications. The flow potential eccentricity is a measure of the curvature of the flow potential. It provides information about the shape and behaviour of the deviatoric plane within the model. The ratio f_{bo}/f_{co} represents the ratio of uniaxial compressive yield stress to the initial uniaxial compressive stress. This ratio is determined using Kupfer's curve for concrete, which provides insight into the material behaviour. The shape of the deviatoric plane is determined by the parameter K, and a value of 0.67 is commonly accepted for this parameter[18]. It influences the stress-strain response and deformation characteristics of the material. The viscosity parameter plays a role in enhancing the convergence rate of the model, particularly when the softening process occurs. It affects the stability and accuracy of the numerical analysis by controlling the rate of strain localization and ensuring a smoother transition during softening. Here we take it as 0.01 for convergence[19].

4.3.1.1. Compressive Behaviour

The stress-strain relationship provides a comprehensive understanding of the compressive behaviour of concrete. However, when experimental data is limited, it becomes necessary to formulate the stress-strain curve using available references such as the Abaqus documentation [17], Eurocode [16], and the fib model code [20] . In this particular case, the only available data was the compressive strength of the concrete, which measured at 14.3 MPa [5].

It is important to note that while analytical data has its limitations when compared to real-world behaviour, it still provides valuable insights. The general stress-strain behaviour, as depicted in figure 4.2, can be divided into three distinct parts according to Eurocode [16]:

Linear Elastic Behaviour: The initial stage of the stress-strain curve exhibits linear elastic behaviour until reaching the initial yield point. During this phase, the concrete deforms elastically, meaning it returns to its original shape once the load is removed.

Plastic Behaviour: After the initial yield point, the stress-strain curve enters the plastic behaviour region. In this stage, the concrete undergoes plastic deformation, showing a hardening behaviour until reaching the ultimate stress. The material continues to deform plastically under increasing stress.

Softening Region: Beyond the ultimate stress, the stress-strain curve enters the softening region. Here, the concrete experiences a decrease in stress as it undergoes additional deformation. This softening behaviour can be attributed to the development of cracks and the degradation of the material's strength. By understanding and characterizing these three regions, a more comprehensive representation of the compressive behaviour of concrete can be achieved. This knowledge is crucial for accurately modelling and analysing concrete structures under compressive loading conditions.

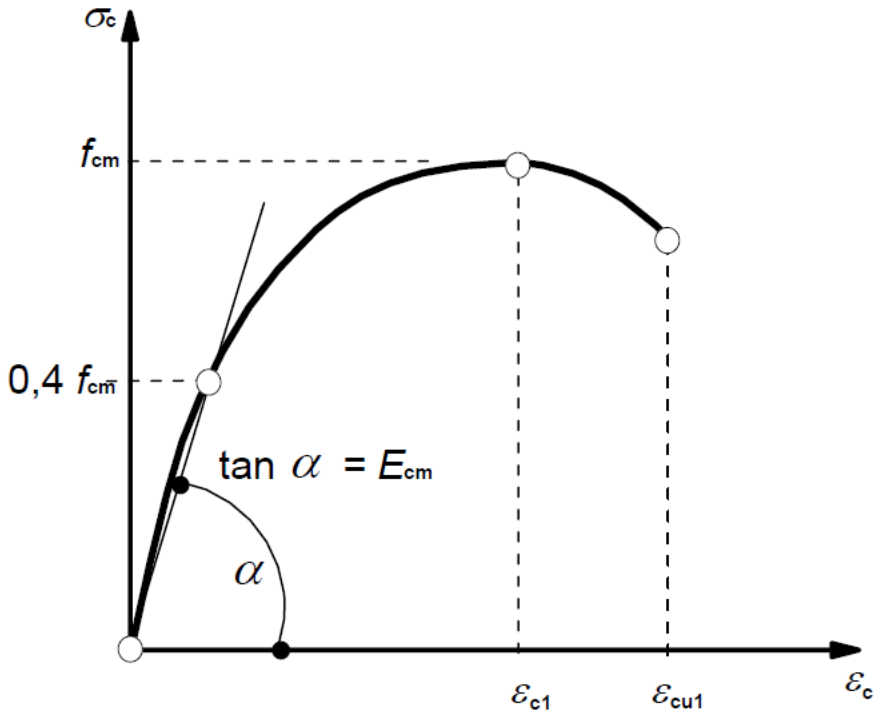

Figure 4.2: Schematic representation of the stress-strain relation for structural analysis (the use of $0.4f_{cm}$ for the definition of E_{cm} is approximate)[16]

The ultimate stress, according to the Eurocode, happens at a strain of 0.002. But it turned out that the analytical data varied from the results of the trial. The load-displacement curve appeared to provide a more realistic portrayal once this was changed to 0.0025.

The elastic behaviour was calculated based on the following relation as shown in Eq. (4.1) [16]:

$$E_{cm} = 22\,[f_{cm}/10]^{0.3} = 24.492\ GPa \qquad (4.1)$$

Where E_{cm} is the mean elastic modulus of the concrete and f_{cm} is the compressive strength of the concrete. The initial elastic behaviour was considered to happen between the stress equal to 0 to a value of 0.4 f_{cm}[16]. The Poisson's ratio for the uncracked concrete is taken as 0.2 [16].

To accurately model the nonlinear behaviour of concrete, the concrete plasticity model requires information on the inelastic strain and corresponding stress values. Additionally, damage parameters for both tension and compression are necessary to calculate the material's response. In this study, an overall approach was adopted to capture the nonlinear behaviour of concrete in both tension and compression. The modelling process was divided into two stages: from the initial yield point to the crushing stress, and beyond that point.

In the initial stage, the focus was on the hardening region, where the concrete exhibits a progressive increase in stress and strain. The behaviour in this region was formulated using appropriate constitutive equations that consider the plastic deformation and hardening characteristics of the material. The model captured the concrete's ability to withstand higher loads and resist deformation up to the point of reaching the crushing stress.

Beyond the crushing stress, the nonlinear behaviour of concrete was further formulated. It can be inferred that this part of the modelling process considered the material's softening behaviour, which occurs after reaching the crushing stress. Softening is typically associated with the development of cracks and the degradation of the material's strength. By implementing these modelling approaches, the study aimed to accurately represent the nonlinear behaviour of concrete in both tension and compression. This allowed for a more realistic simulation of the material's response under various loading conditions and facilitated a comprehensive analysis of concrete structures.:

$$\frac{\sigma_c}{f_{cm}} = \frac{k\eta - \eta^2}{1 + (k-2)\eta} \qquad (4.2)$$

Where:

$$\eta = \varepsilon_c / \varepsilon_{c1} \qquad (4.3)$$

ε_{c1} is the strain at the peak stress- Usually taken as 0.002, but to get a comparable data with the experimental results it was taken as 0.0025.

$$k = 1.05\, E_{cm} \times |\varepsilon_{c1}| / f_{cm} \qquad (4.4)$$

Where the above expression Eq. (4.2) is valid for $0 < |\varepsilon_c| < |\varepsilon_{cu1}|$ where ε_{cu1} is the nominal ultimate strain

Figure 4.3 shows the formulation of the stress-strain curve as per ABAQUS documentation [17] which is required to calculate the damage parameters. Although accurate design of the damage parameter produces results that are similar to reality, the absence of experimental data forces the damage parameter to be calculated theoretically. To input the concrete damage plasticity model apart from the elastic behaviour it is required to calculate the inelastic strain and the damage parameters, which is taken from ABAQUS documentation[17] which is explained below. Hafezolghorani M et.al [21] explained the calculation of concrete compression damage parameter in detail.

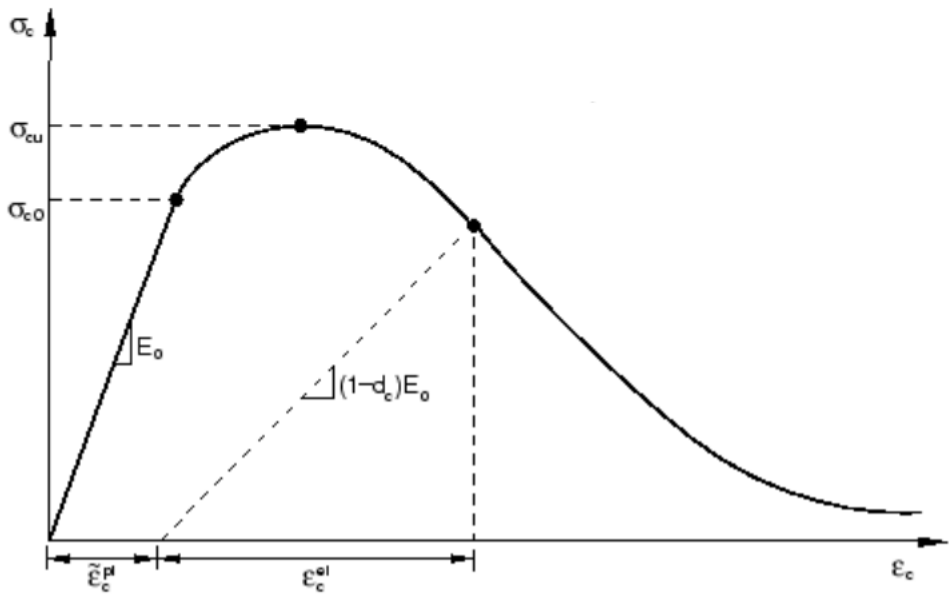

Figure 4.3: Response of concrete to uniaxial loading in compression[17]

$$\varepsilon_c^{in} = \varepsilon_c - \varepsilon_{oc}^{pl} = \varepsilon_c - \frac{\sigma_c}{E_{cm}} \quad (4.5)$$

$$\varepsilon_c^{pl} = \varepsilon_c^{in} - \frac{d_c}{1 - d_c}\frac{\sigma_c}{E_{cm}} \quad (4.6)$$

$$d_c = 1 - \frac{\sigma_c}{f_{cm}} \quad (4.7)$$

Where:

ε_c^{in} – the inelastic strain

ε_c^{pl} – the plastic strain

ε_c – the total compressive strain

ε_{oc}^{el} – the elastic compressive strain corresponding to undamaged material

σ_c- the compressive stress

f_{cm}- the ultimate compressive strength

E_{cm}- the initial undamaged modulus of elasticity

d_c- the concrete damage in compression

Figure 4.4 presents the stress-strain behaviour of concrete in compression, which was analytically calculated. This plot illustrates how the concrete material responds under compressive loading. Table 4.2 provides the input parameters used in the analysis. These parameters include the compressive stress, inelastic strain, and damage parameter, which were calculated based on the equations specified in the study.

The compressive stress represents the magnitude of the applied compressive load on the concrete specimen. The inelastic strain corresponds to the deformation experienced by the material beyond the linear elastic region. It captures the plastic deformation and non-recoverable strains in the concrete.

Table 4.2: CDP input parameter for concrete Compressive behaviour

Compressive Stress, (σ_c) (MPa)	Inelastic strain (ε_c^{in})	Damage compression (d_c)
5.72	0	0
8.19	0.000165	0
11.72	0.000521	0
13.38	0.000954	0
14.11	0.001424	0
14.30	0.001916	0
14.162	0.002422	0
13.79	0.002937	0.01
13.27	0.003458	0.04
12.63	0.003984	0.07
11.91	0.004514	0.12
11.13	0.005046	0.17
10.29	0.00558	0.22
9.41	0.006116	0.28
8.50	0.006653	0.34
7.56	0.007191	0.41
6.59	0.007731	0.54

Additionally, the damage parameter is determined to quantify the level of damage or degradation occurring in the concrete as it undergoes compressive loading. This parameter indicates the extent of cracking or weakening in the material, which affects its overall strength and behaviour. By utilizing the analytically calculated stress-strain behaviour and the input parameters listed in Table 4.2, the study aimed to accurately model and analyse the compressive behaviour of concrete. The damage parameter until 0.54 showed to be reasonable with the experimental curve. Beyond that the degradation was too

much which caused noise in the model. So, an accurate experimental data is required to model the damage parameters precisely.

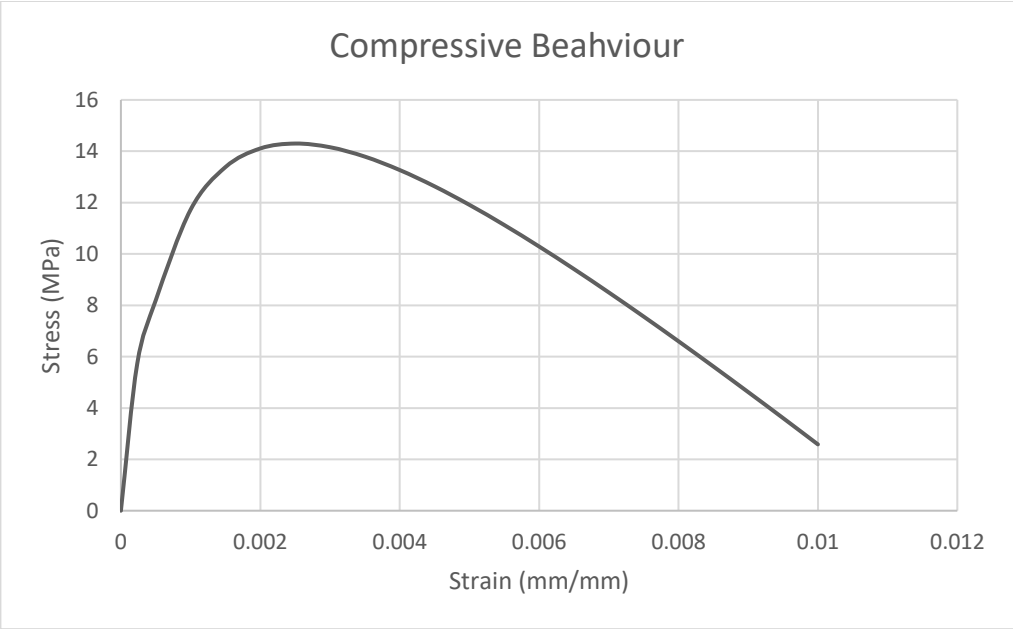

Figure 4.4: Stress-strain curve as calculated per Eurocode-2

4.3.1.2. Tensile Behaviour

To complete the Concrete Damage Plasticity (CDP) model, it is necessary to consider the tensile behaviour of concrete. This aspect plays a crucial role in accurately capturing the material's response under tension. In the CDP model implemented in Abaqus, three alternative methodologies are available to model concrete damage in tension. These methodologies include considering the tensile strength in conjunction with either strain, crack opening displacement, or fracture energy.

Among these alternatives, the relationship between cracking stress and strain has shown to be particularly effective in analysis. By using this approach, the stress-strain relationship in concrete's tensile behaviour can be divided into two distinct parts. The first part is the linear region, which extends until the cracking stress. In this region, the concrete exhibits a linear response, behaving elastically under tension. The relationship between stress and strain follows Hooke's Law.

The second part is the softening branch, which occurs after the cracking strain. In this region, the concrete experiences degradation in strength and stiffness due to the development and propagation of cracks. The

stress-strain relationship in this phase shows a decreasing trend as the material undergoes further deformation.

By incorporating these two regions, the CDP model in Abaqus aims to accurately simulate the tensile behaviour of concrete. The cracking stress and strain relationship, in particular, has proven to be fruitful in capturing the realistic response of concrete structures subjected to tension. There are different models to calculate the tensile strength of the concrete. M.P. Collins et.al [22] proposed a stress-strain relationship for cracked concrete (Eq. (4.8)) who calculated the cracking stress as follows:

$$f_{tm} = 0.33\sqrt{f_{cm}} = 1.24\ MPa \tag{4.8}$$

Where f_{tm} is tensile strength of the concrete. But the analytical equation implemented was not showing enough capacity for the concrete and through calibration a tensile cracking strength of 2.25 MPa gave more aligned to the experimental value. The softening behaviour post the cracking strain is modelled using the following correlation (Eq. (4.9)) explained by Mei S et.al. [23]:

$$\sigma_t = \frac{f_{tm}}{1 + \sqrt{500\ \varepsilon_t}} \tag{4.9}$$

Where:

σ_t - the tensile stress

ε_t – the total tensile strain

In a similar fashion as explained earlier, the ABAQUS documentation provides the tensile behaviour (Figure 4.5) of the concrete and the tensile damage variable (d_t) is calculated as follows:

$$\varepsilon_t^{in} = \varepsilon_t - \varepsilon_{ot}^{pl} = \varepsilon_t - \frac{\sigma_t}{E_{cm}} \tag{4.10}$$

$$\varepsilon_t^{pl} = \varepsilon_t^{in} - \frac{d_t}{1 - d_t}\frac{\sigma_t}{E_{cm}} \tag{4.11}$$

$$d_t = 1 - \frac{\sigma_t}{f_{tm}} \qquad (4.12)$$

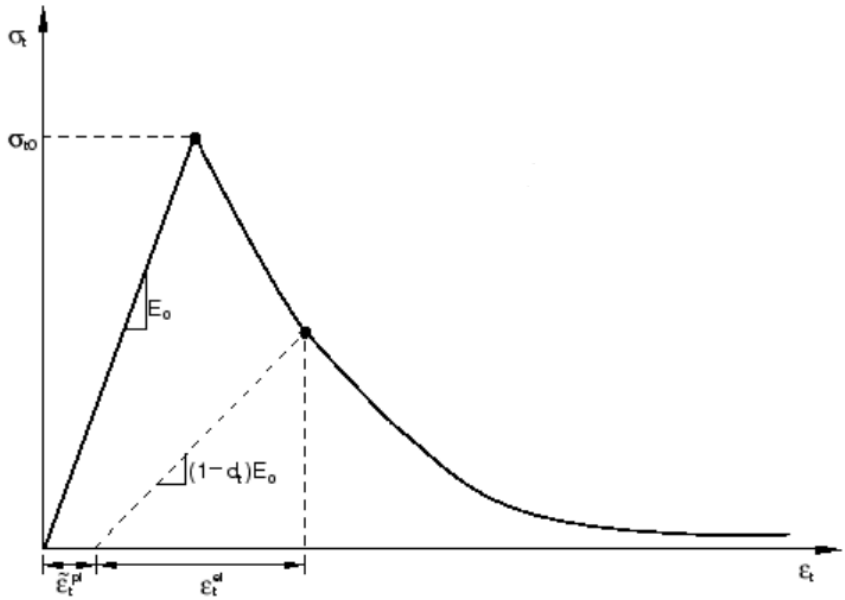

Figure 4.5: Response of concrete to uniaxial loading in tension [17]

Based on the above correlation the tensile stress-strain behaviour implemented in the CDP model is shown in figure 4.6. The table 4.3 shows the values of cracking strain, stress and the damage variables.

Table 4.3: CDP input parameter for concrete tensile behaviour

Tensile Stress, (σ_t) (MPa)	Inelastic strain (ε_t^{in})	Damage tension (d_t)
2.25	0	0
1.621857	0.000208133	0.279175
1.586373	0.000258133	0.294945
1.554712	0.000308133	0.309017

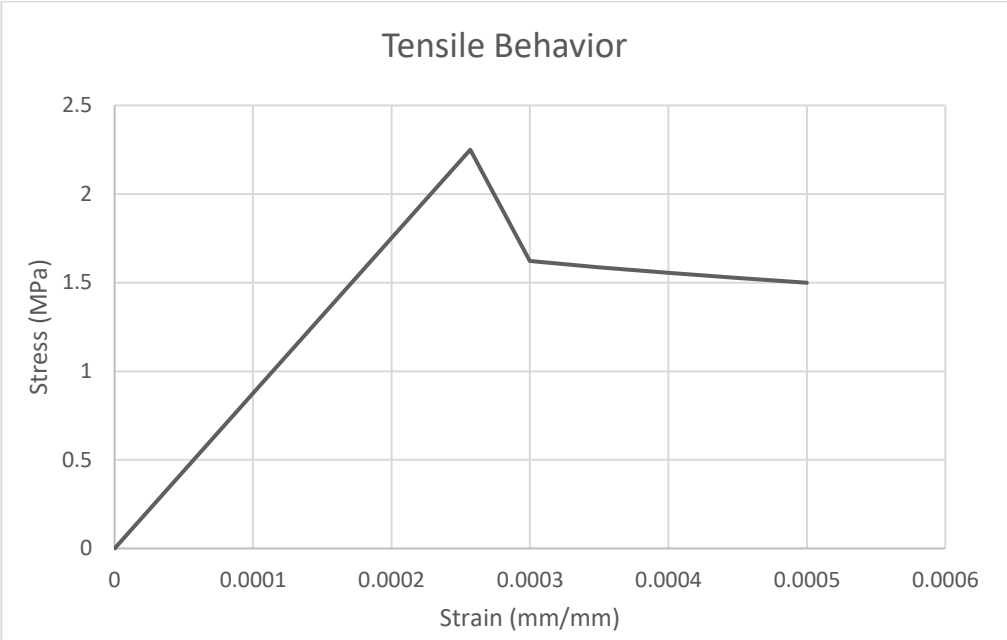

Figure 4.6: Response of concrete to uniaxial loading in tension [17]

In the context of concrete tension behaviour, it has been observed that the degradation of the damage parameter beyond a value of 0.3 resulted in a significant decrease in the capacity of the column. This finding suggests that modelling the damage parameter in a more accurate and representative manner can lead to improved results comparable to experimental scenario. By accurately modelling the damage parameter, taking into account the degradation beyond the critical value of 0.3, a more realistic representation of the concrete's behaviour under tension can be achieved. This improved modelling approach can enhance the accuracy of the simulation and provide better agreement with experimental results.

4.3.2. Steel

In the experimental study [5], deformed bars were used as steel reinforcement. The longitudinal reinforcement was arranged according to figure 4.7, where sides A and C had five longitudinal reinforcement bars each, while sides B and D lacked longitudinal reinforcement. The stirrups, which provided transverse reinforcement, were also included in the model following the experimental setup which had a diameter of 8 mm.

To define the behaviour of the steel reinforcement in the model, elastic properties were assigned based on the material's characteristics. For simplicity, a simplified plasticity model was introduced, following the guidelines outlined in model code 2010 [20] . The yield stress for both the transverse and longitudinal reinforcement was assumed to be 531 MPa for ease of modelling and analysis. The ultimate strain value was taken as 0.1 as per the fib model code 2010 [20] .

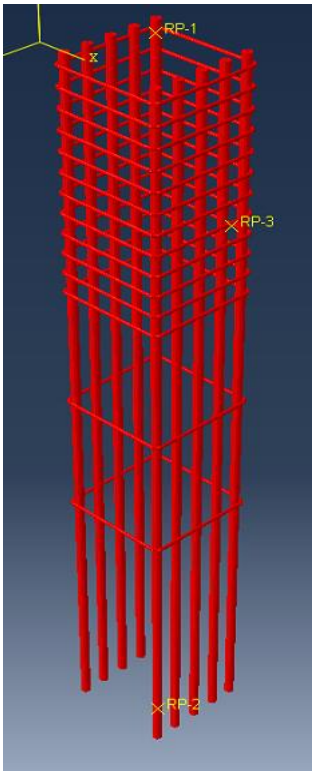

Figure 4.7: Steel reinforcement

Table 4.4 and 4.5 provide detailed information about the elastic and plastic behaviour of the steel reinforcement, respectively. The elastic properties describe the steel's response within the linear elastic range, while the plastic behaviour accounts for the material's nonlinear response and plastic deformation. In this study, an isotropic hardening behaviour was chosen to represent the steel reinforcement's response under monotonic loading. It is important to note that while there are multiple hardening laws available in Abaqus, for monotonic loading, they yielded similar outputs. Therefore, the isotropic hardening behaviour was selected for its simplicity and practicality in this particular analysis.

By accurately modelling the steel reinforcement using its elastic and plastic properties, the study aimed to capture the behaviour and contribution of steel reinforcement in the structural response of the concrete

column. This enabled a comprehensive analysis of the interaction between the concrete and steel components and their combined performance under loading conditions. Figure 4.8 provides the stress-strain behaviour of the steel.

Table 4.4 : Elastic behaviour of steel

Modulus of Elasticity, E_s (GPa)	Poisson's ratio, ν	Density (tonnes/mm³)
200	0.28	7.85E-09

Table 4.5 : Plastic behaviour of steel

Yield stress (MPa)	Plastic strain
531	0
531	0.1

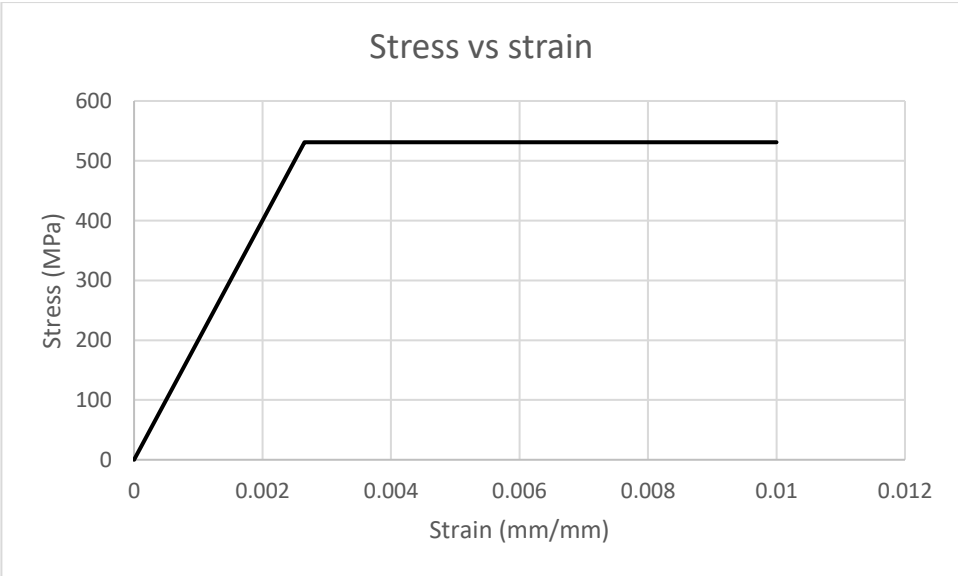

Figure 4.8: Stress-strain behaviour of steel

4.3.3. CFRP

The properties of the CFRP (Carbon Fiber Reinforced Polymer) laminate were input into the analysis without considering any damage. Therefore, only the elastic behaviour of the CFRP material was taken into account. However, due to the absence of certain properties, data was obtained from the paper authored by Sun Q et.al. [24] to supplement the missing information.

Table 4.6 presents the details of the properties of the CFRP laminate, which were derived from the mentioned paper. This table provides important information such as the modulus of elasticity, Poisson's ratio, and other relevant properties that are crucial for accurately modelling the behaviour of the CFRP material. By incorporating the properties outlined in Table 3.6, the analysis aims to simulate the response of the CFRP laminate and its interaction with the concrete material only considering the elastic behaviour of the CFRP.

Table 4.6: CFRP Properties

E_1 (MPa)	$E_2 = E_3$ (MPa)	ν_{12} (MPa)	G_{12} (MPa)	G_{23} (MPa)
252000	20394	0.29	30067	6100

4.4. Loading and Boundary Conditions

Loading protocol was defined as same as the one presented in the paper [5]. The short columns are subjected to a constant compressive load and a horizontal cyclic displacement. As the numerical study is analysing the envelope of the hysteresis curve the loading protocol was replaced from cyclic to monotonic condition. The axial compressive load of 1.43 MPa was applied constantly on the top surface of the short column as shown in figure 4.9. The horizontal displacement was applied at a distance of 900 mm from the base cross-section.

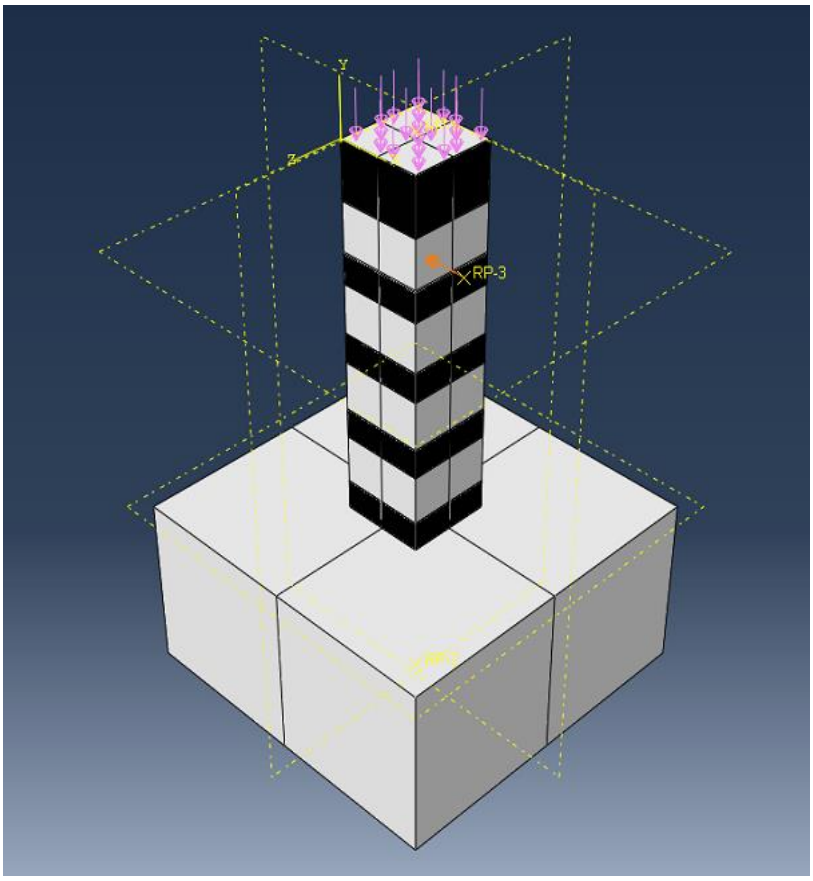

Figure 4.9: Loading and boundary condition

In the numerical study being conducted, a monotonic loading condition is employed. To simulate the monotonic loading condition, the total time period of the cyclic loading protocol, which is 4946.4 seconds, is used as the duration for the monotonic loading. The cyclic loading condition explained in the experimental studies was converted to a comparable monotonic pushover. The rate of displacement applied was equal in all stages of monotonic loading with respect to the experimental loading protocol (explained in section 3.2.2). Until the time reached 1404 seconds, a loading rate of 0.2 mm/s was adopted and from time 1404 seconds to 3391.2 seconds a loading rate of 1.0 mm/s was adopted and after that until the time equals 4946.4 s the loading rate was 2.0 mm/s. The loading was implemented in ABAQUS by defining an amplitude protocol for correctly implementing the experimental loading rate. That is for example in the second cycle 1.78 % of the final displacement, 100.8 mm was implemented which results a displacement of 1.8 mm provided at a rate of 0.2 mm/s.

In the numerical study, displacement control is applied to replicate the same rate at which the cyclic loading was performed during the experimental study. The details of the monotonic loading protocol implemented in the numerical analysis can be found in table 4.7 and figure 4.10. These provide a comprehensive description of the specific loading parameters and the corresponding displacement control rates used in the numerical simulations.

By following this monotonic loading protocol, the numerical study aims to replicate the loading conditions and evaluate the behaviour and response of the concrete column under monotonic loading. This allows for a comparison between the experimental cyclic loading behaviour and the numerical monotonic loading behaviour, providing insights into the performance of the column under different loading scenarios.

Table 4.7: Abaqus load protocol for monotonic loading

Time	Amplitude	Displacement
0	0	0
108	0.017857	1.8
324	0.035714	3.6
756	0.071429	7.2
1404	0.107143	10.8
1576.8	0.142857	14.4
1836	0.214286	21.6
2181.6	0.285714	28.8
2700	0.428571	43.2
3391.2	0.571429	57.6
3823.2	0.714286	72.0
4341.6	0.857143	86.4
4946.4	1	100.8

The lateral load was applied on the reference point, RP 3. This reference point was then kinematically coupled with the shear length in which the details of interaction between the reference point and the load application point is described in detail in section 4.7.

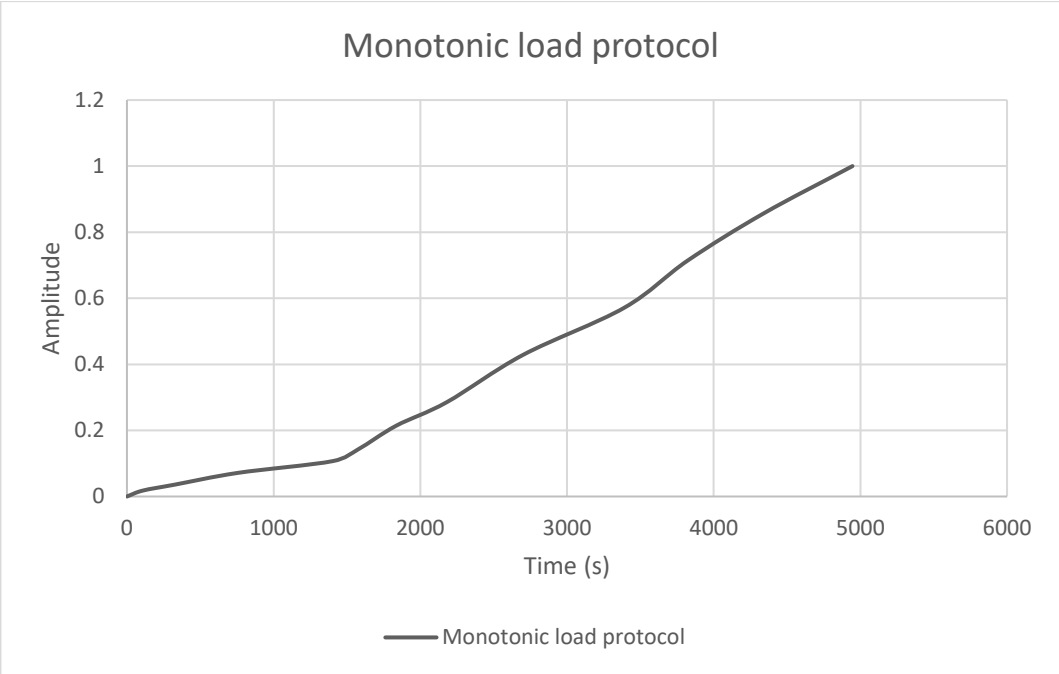

Figure 4.10: Abaqus load protocol

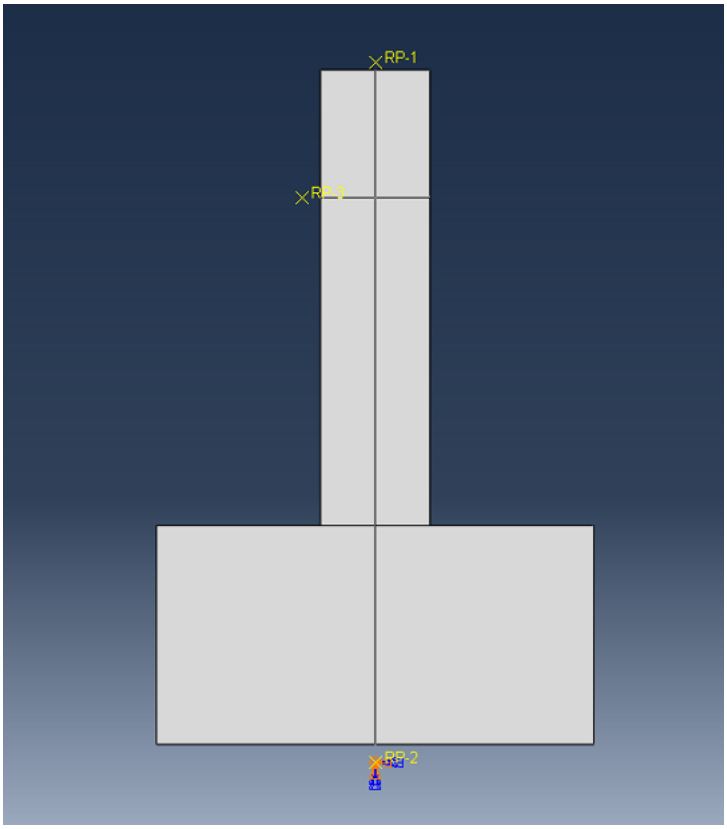

Figure 4.11: Boundary condition

The boundary conditions in the numerical analysis were set up to replicate the experimental setup precisely. In the experimental model, the base of the column was fixed, and this condition was replicated in the numerical model as well. To achieve this, the base of the column was fixed at a reference point RP-2. This RP-2 was kinematically coupled with the base plane of the foundation block. This coupling method allows for the calculation of history outputs without the need for additional calculations for the reaction forces after the analysis. The advantage of this approach is that it provides more accurate results (figure 4.11). By replicating the experimental boundary conditions accurately and employing this kinematic coupling method, the numerical analysis aims to capture the behaviour and response of the concrete column more effectively, leading to more accurate and meaningful results.

4.5. Mesh

Different element choice and selection of the element type for meshing accurately helps to simulate the behaviour. The proper element selection for each type of model helps to get a correct response. In this study majorly 3 types of elements were used. One solid element, truss element and a shell element (figure 4.12).

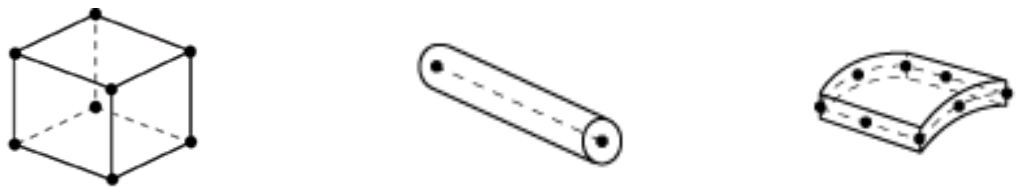

a) Solid element b) Truss element c) Shell element

Figure 4.12: Different element type[17]

For concrete C3D8R, an 8-node linear brick, reduced integration, hourglass controlled element was used. For CFRP, S4R, A 4-node doubly curved thin or thick shell, reduced integration, hourglass control, finite membrane strains are used with a global mesh size of 10 mm. Whereas for the longitudinal and transverse reinforcement a T3D2 element type (A 2-node linear 3-D truss) is used with for modelling. The meshed model of the CFRP strengthened (S4) is shown in figure 4.13. The as-built specimen has the same mesh properties except for the CFRP one.

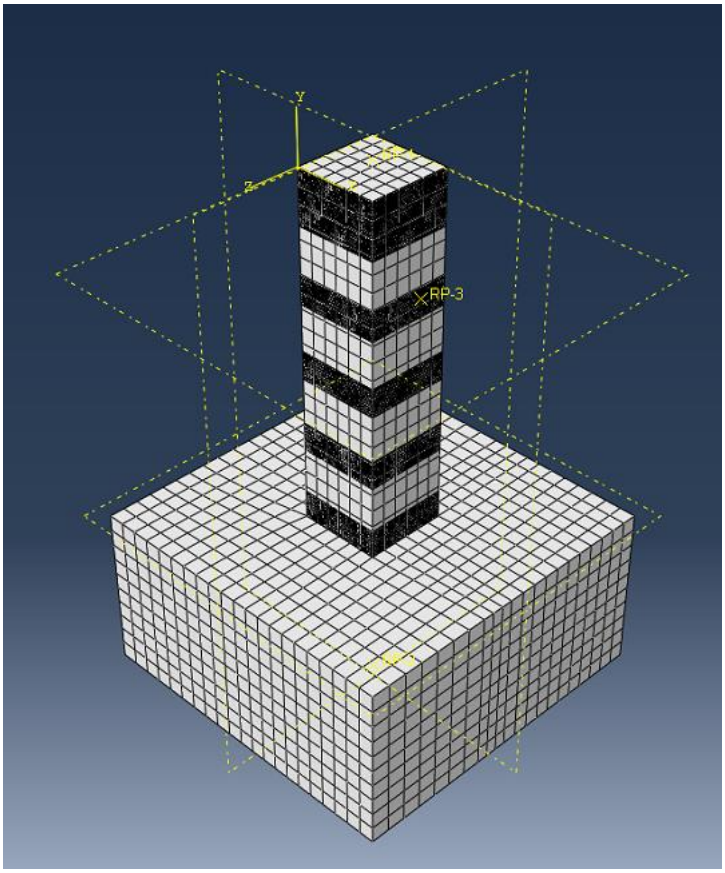

Figure 4.13: Meshed model

4.5.1. Concrete

As explained above concrete is modelled with solid element, C3D8R. The C3D8R (continuum /solid) element is specifically designed as a reduced integration element, which means that it utilizes fewer integration points compared to the fully integrated counterparts (such as the C3D8 element). This reduced integration scheme provides computational efficiency while maintaining reasonable accuracy in the analysis results. While using reduced integration there might happen an hourglass issue[17]. Hour glassing, also known as hourglass mode or hourglass instability, refers to a spurious mode of deformation that can occur in certain finite element analysis simulations in solid elements. In stress/displacement analysis, hour glassing can be a concern with first-order, reduced-integration elements. The elements can distort to the point that the strains estimated at the integration point are all zero because they have a single integration point, which results in an uncontrolled distortion of the mesh. So, to avoid this the C3D8R element includes an hourglass control mechanism to the instabilities in the analysis. This

hourglass control helps maintain numerical stability and prevents unrealistic deformations during the simulation. The average mesh size used was 60 mm for the concrete column.

4.5.2. Steel reinforcement

T3D2 is a three-dimensional truss element with 2 nodes of integration. It is primarily used for modelling one-dimensional structural members, such as trusses, beams, and cables, bars etc. For simplicity in designing the steel reinforcement and assuming there is no relative movement between steel and concrete a truss element seems to be a good choice. While modelling a truss element the cross-sectional area can be defined to recreate the steel reinforcement cross-sectional area. For both the longitudinal and transverse reinforcement the T3D2 element type is used. A global mesh size of 10 mm was used in the case of both transverse and longitudinal reinforcement.

4.5.3. CFRP

The S4R element is a four-node linear shell element with reduced integration. The comparatively thin CFRP plate was modelled using shell elements. For CFRP a conventional shell was assigned for the section. Conventional shell elements are made primarily to represent thin shell structures with a significant surface area compared to their thickness, like plates and shells. It is a continuum element that can capture both linear and nonlinear material behaviour, making it suitable for a wide range of structural analysis applications. Without explicitly modelling the interior, these features offer an effective technique to portray the behaviour of these structures. In a similar fashion as explained above a global mesh size of 10 mm was used for modelling the CFRP strips.

4.6. Interaction

The interaction between the concrete and different reinforcement is helps to capture the behaviour of the concrete accurately. Apart from the usual interaction between concrete and reinforcements (figure 4.14) there were some other interactions between some reference points and the whole assembly. The latter part was used to apply the load and boundary condition in a way so as to extract the history output in a convenient way which will reproduce the load-displacement curve. So broadly the interaction in this study was classified into three- interaction between concrete and steel reinforcement, interaction between concrete and CFRP and the interactions used for extracting the results.

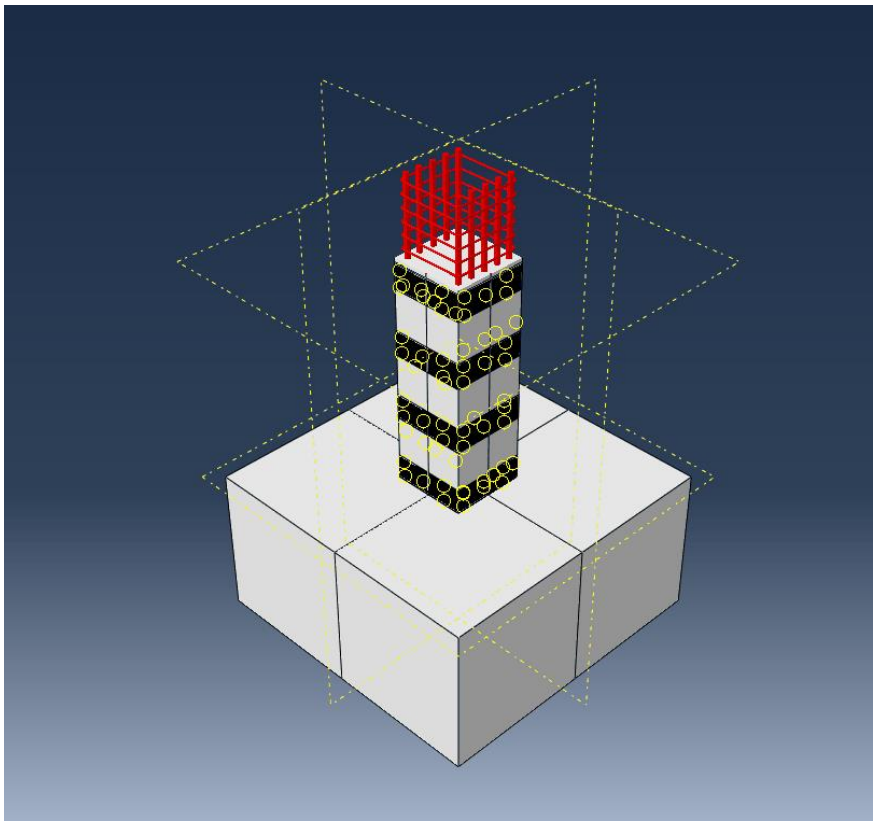

Figure 4.14: Interaction between concrete, steel and CFRP

4.6.1. Interaction between concrete and steel reinforcement

The accuracy of simulating reinforced concrete sections depends critically on the contact between the concrete and internal steel reinforcements. The interface between the concrete and the steel reinforcement was modelled using the embedded elements technique. The host and embedded elements must be identified in the embedded elements method. For illustration purposes, internal steel reinforcements are designated as an embedded region and concrete is shown as the host region[17]. This technique aligns the embedded element nodes with the host region nodes in order to limit the degree of freedom for translation of the embedded nodes.

4.6.2. Interaction between concrete and CFRP

When modelling the interaction between the concrete and CFRP (Carbon Fiber Reinforced Polymer), there are two methods that can be followed: one with perfect bonding and another with the consideration of debonding effects using a cohesive interaction. In the case of perfect bonding, it is assumed that there is no debonding between the CFRP and the concrete. This approach simplifies the model and assumes that

the bond between the two materials is strong and continuous throughout the analysis. To represent this perfect bonding, a tie connection is used in the modelling process. The tie connection acts as a rigid link between the CFRP and the concrete, ensuring that they behave as a single entity.

However, it is important to note that in reality, debonding can occur between the CFRP and the concrete due to various factors such as applied loads, material properties, and interface conditions. This debonding can significantly affect the behaviour and performance of the CFRP-strengthened structure.

In the present study, due to the complexity of modelling the debonding process and the absence of experimental data regarding debonding, it was assumed that the bonding between the CFRP and the concrete is perfect. This simplification allows for a more straightforward analysis, focusing on the behaviour of the CFRP-strengthened structure with a continuous bond.

By considering the perfect bonding assumption and utilizing tie connections, the study aims to capture the overall behaviour and response of the CFRP-concrete interaction, providing insights into the effectiveness of CFRP strengthening in enhancing the structural performance.

4.6.3. Interactions for extracting the history output

As explained in section 4.6 the loading and boundary conditions were applied to some reference points. These reference points were then coupled to the respective surfaces where the load and boundary conditions needed to be applied. The reference points were created to extract the history output and apply the loading and boundary conditions. The reference point RP-1 was used to extract the displacement history output which was coupled kinematically with the top surface (Figure 4.15 a). The reference point 3 (RP-3) was coupled at the shear length where the lateral load displacement was given (Figure 4.15 b). The reference point RP-2 was used to couple with the base surface where the column was fixed (encasterd) where the reaction force output was extracted.

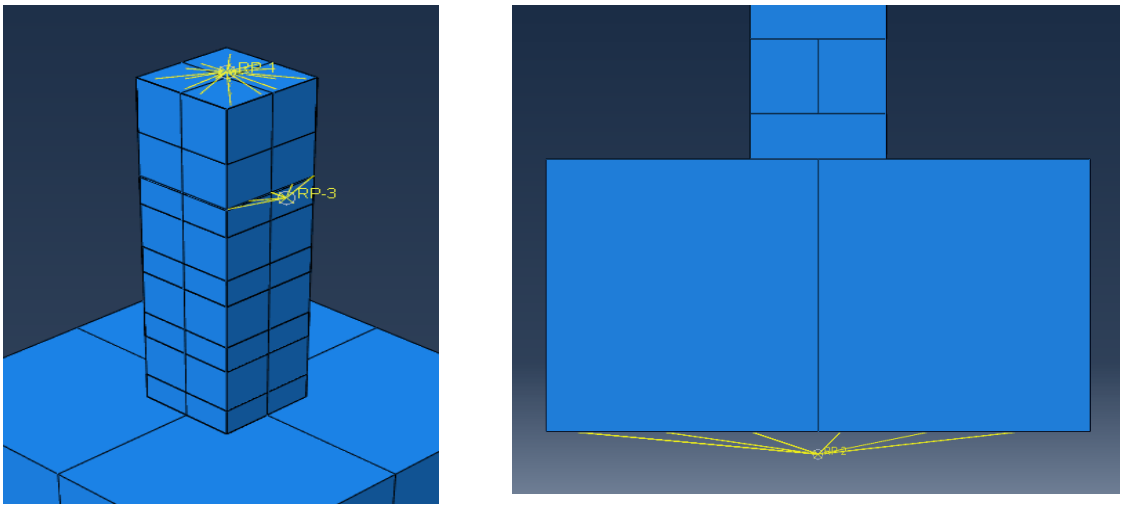

a) Load application and Displacement output

b) Boundary condition application

Figure 4.15: Interactions for extracting the history outputs

All the reference points were used with kinematic coupling. In Abaqus, the term "kinematic coupling" refers to a method for enforcing particular displacement or velocity relationships among various elements or areas of a model during a simulation. It makes it possible to couple degrees of freedom between various regions, which makes it possible to describe intricate interactions and boundary conditions. When examining structures with touch, sliding, or other interactions, this method is especially helpful.

5. RESULTS AND DISCUSSIONS

5.1. Introduction

The present research compares the findings of the Finite Element (FE) analysis carried out in this specific study with the research carried out by Del Zoppo et al. [5], as described in section 3.3 of their work. The static general method, which is regarded as an analytical method that is unconditionally stable, was used in the FE analysis in this study The results are categorized into majorly four categories:

1. The load-displacement curve
2. Crack propagation
3. Stress in steel
4. Strain in CFRP (only in specimen S4)

All the above categories were compared for the as-built specimen and the specimen strengthened with CFRP. And a comparative study is conducted in this chapter. The numerical studies observed had a slight variation with the experimental results. This was expected due to the fact that the material properties were calculated analytically.

5.2. As-Built Specimen

The as-built specimen was examined using the static general method, as mentioned previously. The analysis was performed for different dilation angles, and it was found that a dilation angle of 30° demonstrated better alignment with the experimental results. In the analysis of the as-built specimen, three aspects were investigated: the load-displacement curve, the crack pattern, and the stress in the longitudinal steel reinforcement.

5.2.1. Load displacement curve

The concrete damage plasticity model was subjected to model verification by calibrating the dilation angle specifically for the as-built model, as mentioned earlier. Figure 5.1 displays a comparison between the

experimental data and the numerical model. Notably, the elastic region of the model aligns well with the experimental results. The model was able to capture the non-linear behaviour of the column, the lateral stiffness and the peak capacity.

The calibration of the dilation angle was limited to a maximum of 30 degrees. As the dilation angle exceeded this limit, the numerical model deviated from the characteristic behaviour observed in the experimental data. On the other hand, decreasing the dilation angle below 30 degrees introduced significant noise into the model due to numerical instability.

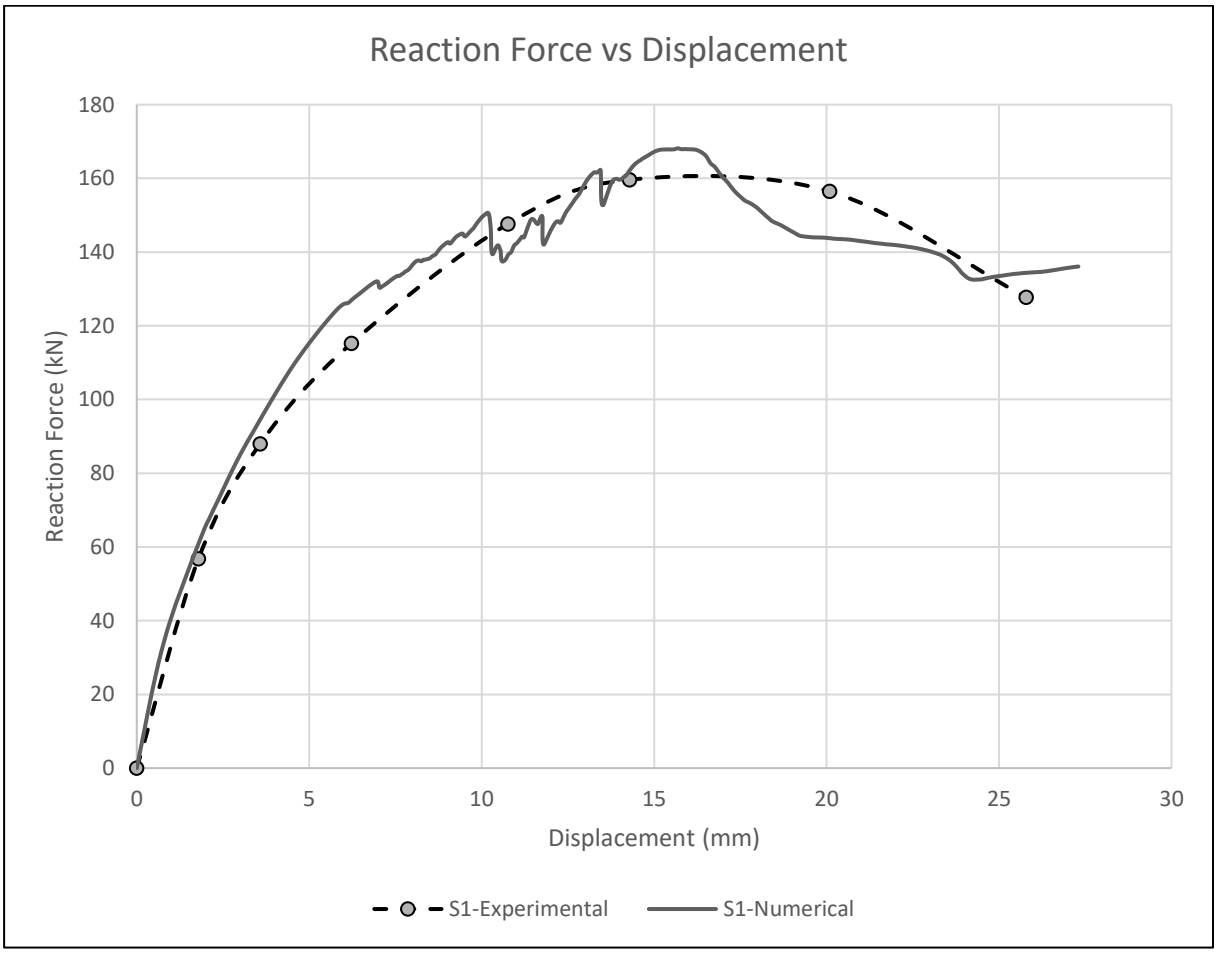

Figure 5.1: Reaction force vs displacement- As-built specimen

The experimental data provided a maximum capacity of 159 kN at a displacement of 14.29 mm. Whereas the numerical model exhibited a maximum load of 168.15 kN at a displacement of 15.69 mm. The percentage deviation of peak force was around 5.4 % whereas the deviation in displacement was around 8.9 % which shows that the FE model was able to capture the shear failure.

5.2.2. Crack Pattern

In order to analyse the propagation of crack openings, the output parameter PEEQT, which refers to tensile equivalent plastic strain or cracking strain, was utilized [25]. Figure 5.2 illustrates a comparison of the crack patterns on side D between the experimental (figure 5.2 a) and numerical models (figure 5.2 b). The finite element (FE) model successfully captures the location of the crack. However, the accuracy of crack capture can be further enhanced through mesh refinement. Unfortunately, due to limitations in system capacity, it was not possible to employ a finer mesh for analysis. Additionally, a more accurate modelling of the damage parameter could improve the representation of the crack pattern.

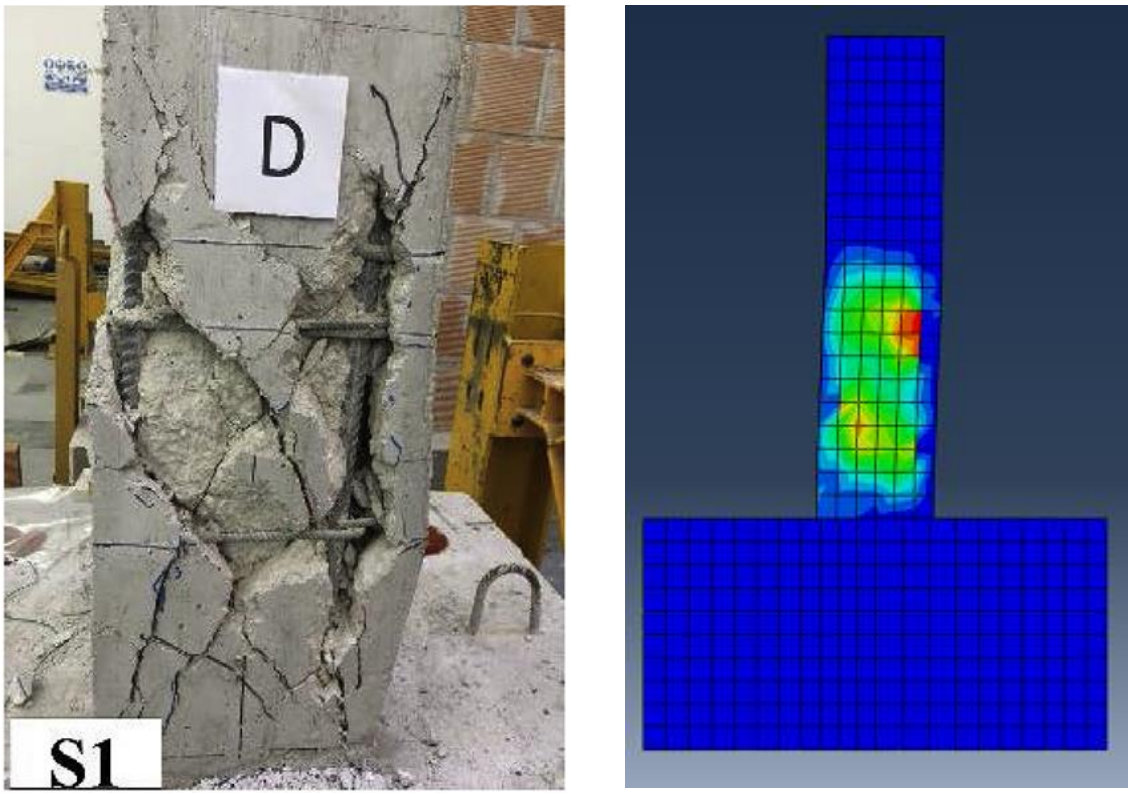

a) Experimental [5] b) Numerical

Figure 5.2: Crack pattern comparison

The cracks observed on sides B and D in the experimental scenario were attributed to the absence of longitudinal reinforcement, which was also reflected in the numerical model. This alignment of results with the experimental observation reinforces the validity of the numerical model in capturing the behaviour of cracks.

5.2.3. Stress in Steel Reinforcement

In the case of the as-built model, the experimental results indicated a brittle failure, suggesting that the steel reinforcement did not reach its full capacity. Unfortunately, the experimental study did not provide any data regarding the stress in the steel reinforcement. However, through analysis of the numerical model, it was observed that the stress in the steel, particularly close to the peak load, was significantly lower than the capacity of the steel. This implies that the steel reinforcement was not fully utilized, and the failure of the column was primarily governed by brittle shear failure.

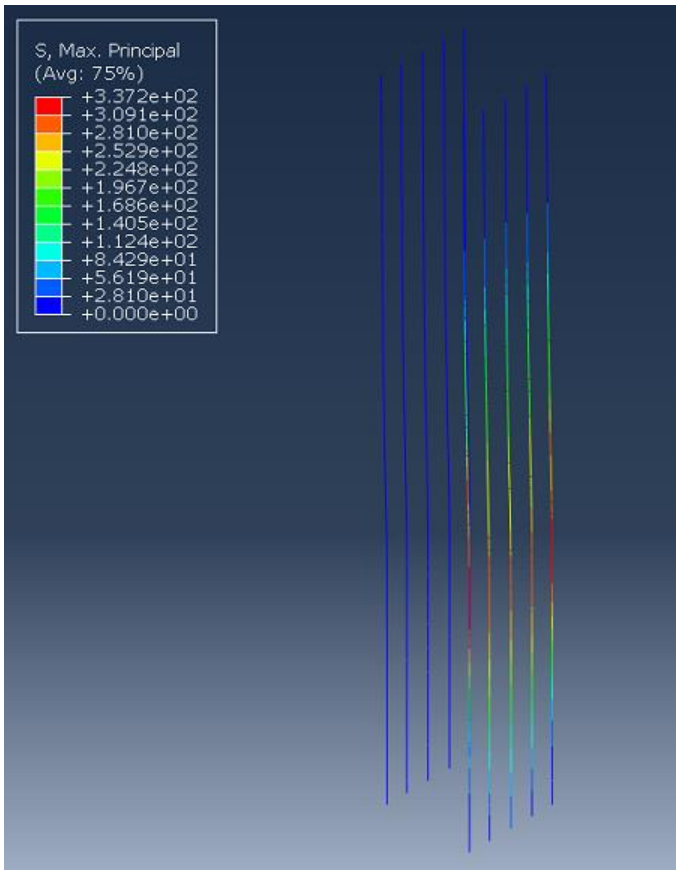

Figure 5.3: Maximum principal stress at the peak load

Figure 5.3 presents the maximum principal stress in the longitudinal reinforcement, which was measured to be 337.2 MPa. It is important to note that the capacity of the steel, represented by its yield stress, was 531 MPa. This stark difference indicates that the column failed due to shear failure rather than flexural failure.

5.3. CFRP Strengthened Specimen

5.3.1. Load displacement curve

The numerical study of CFRP strengthened specimen showed that the capacity was only reached when the dilation angle was increased to 55 degrees [26]. The dilation angle, which is the ratio of volume strain to shear strain, plays a crucial role in determining the ductility and overall behaviour of the model. An increase in the dilation angle leads to greater flexibility in the system. This means that as the dilation angle increases, the material becomes more capable of undergoing plastic deformation and can accommodate larger strains. From a practical perspective, an increase in the internal dilation angle has several effects. Firstly, it results in higher plastic strains, meaning that the material can undergo larger deformations before failure. Secondly, it leads to increased confining pressure, which provides additional support and restraint to the material, enhancing its strength and resistance to failure [18]. These effects are important considerations in engineering applications, as they impact the overall behaviour and response of structures under loading conditions. Despite the fact that the dilation angle of the as-built specimen was 30°, the FRP confinement increases the column's capacity, which in turn changes the dilation angle. Thus, with calibration a dilation angle of 55° was chosen to be more realistic with the experimental observation.

The peak value of experiment showed around 286.66kN at a displacement of 21.46 mm. Whereas in the case of the numerical model it showed that the first peak was obtained at a displacement of 21.98 mm with a peak load of 289.88 kN. This is comparable to the experimental result.

Figure 5.4 compares the load-displacement curve for experimental and numerical model. The numerical model was approached in two ways, the CFRP was considered as lamina and as an isotropic material due to convergence issues. The assumption of isotropic material for CFRP is obviously not realistic; however, given the geometric arrangement of the uniaxial CFRP strips it is reasonable to consider that the strips are not able to develop significant stresses in their transverse direction. However, further analyses are required to fully model the post-peak behaviour of CFRP strengthened specimens. The high numerical instability can be overcome by using an explicit analysis, but due to its time-consuming nature and conditional stability it requires high-performance computing systems.

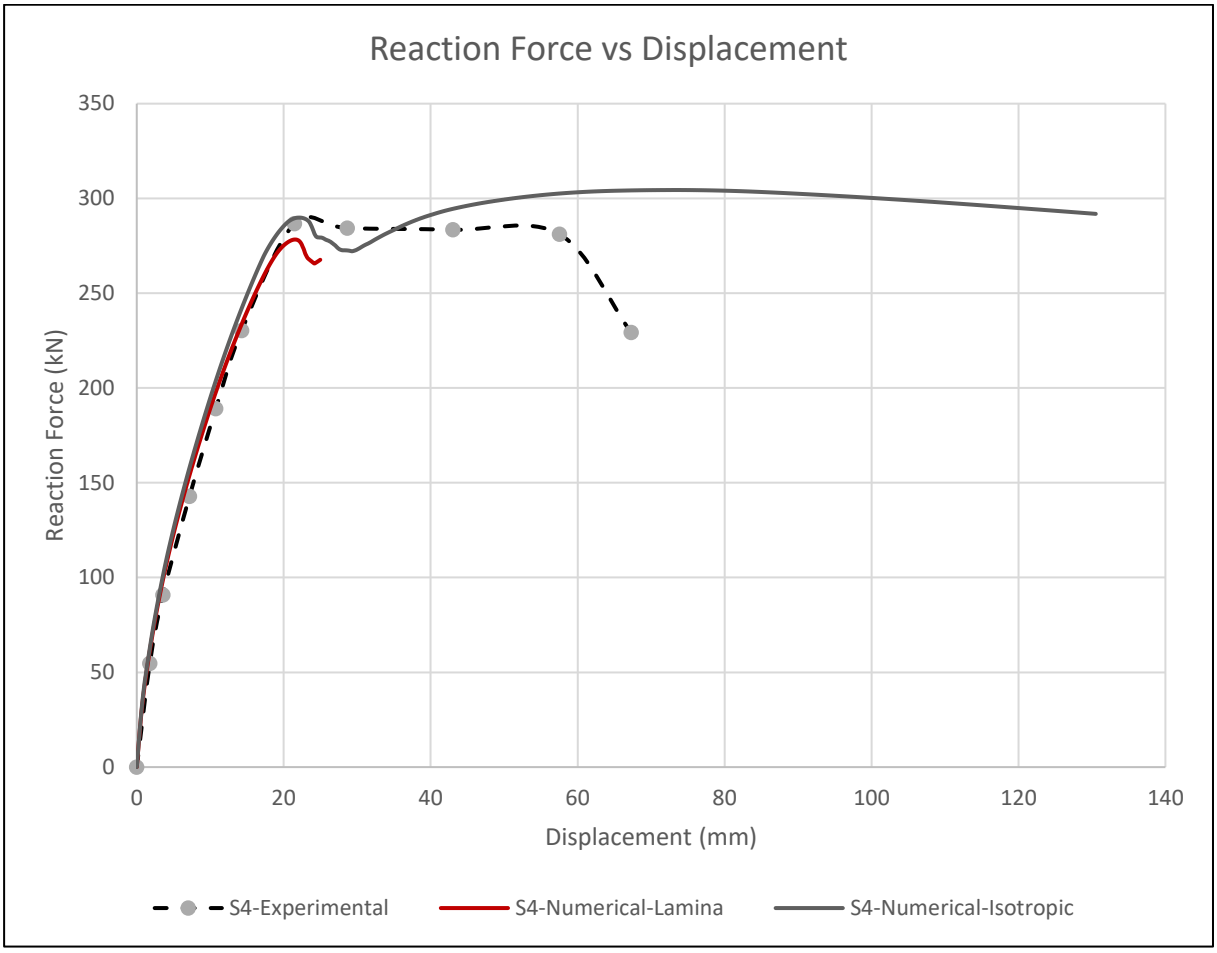

Figure 5.4: Reaction force vs displacement- CFRP strengthened specimen

5.3.2. Crack Pattern

The specimen strengthened with CFRP in experiment exhibited a quasi-ductile behaviour. The damage was not that extensive. The lateral capacity was dropped suddenly due to the CFRP rupture in the third strip. From the experimental figure we can see that there was a degradation in concrete where the confinement strips were not present. In a similar fashion the damage was mostly concentrated in concrete present between the CFRP strips. This indicates a comparable behaviour between CFRP strengthened specimen in experimental and numerical model (figure 5.5).

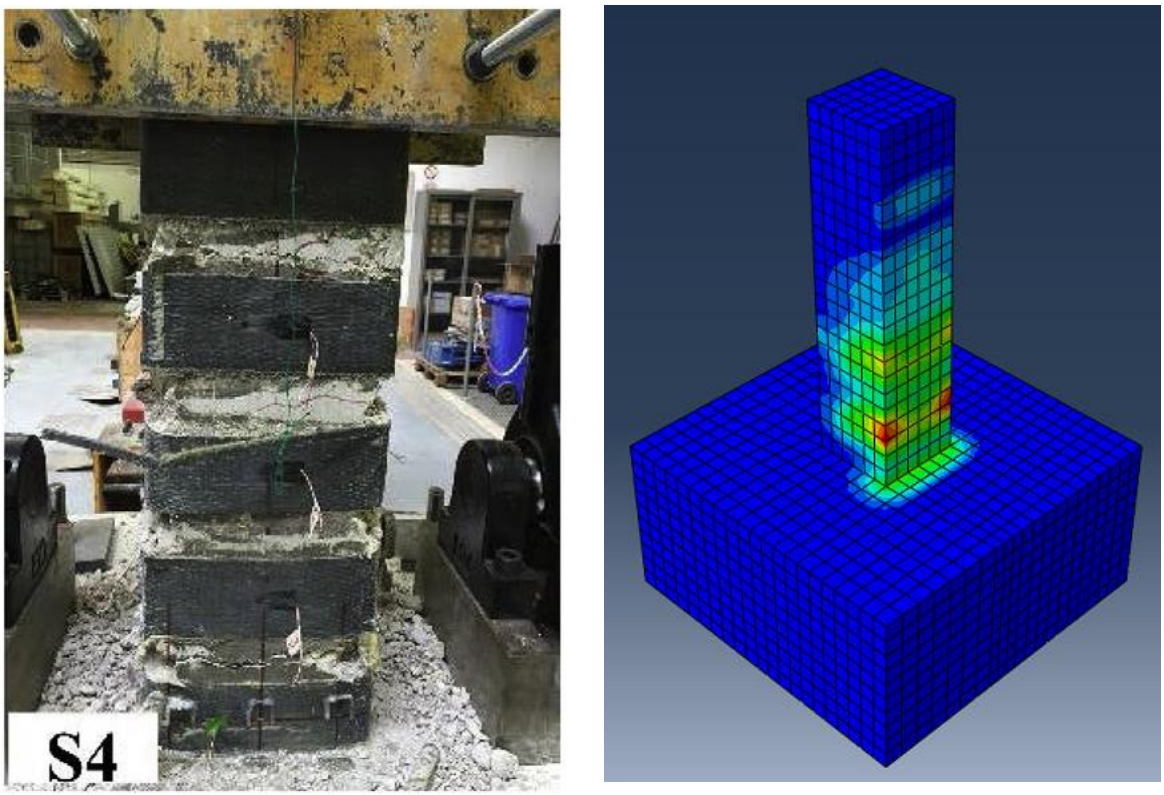

a) Experimental b) Numerical

Figure 5.5: Crack pattern/ damage of concrete

5.3.3. Stress in Steel Reinforcement

As opposed to the as-built specimen, the longitudinal steel reinforcement reached its yielding capacity before reaching the peak load. This shows that the CFRP confinement has worked to prevent a brittle failure and has assisted steel to reach its yield point. This indicates that the failure mode is shifted from the brittle to ductile failure. As per the experimental results obtained with CFRP strengthened specimen, it exhibits ductile performance. The numerical analysis showed that the steel has reached its yield capacity of 531 MPa (figure 5.6), before reaching the peak force, which shows a ductile behaviour in case of CFRP strengthened specimen.

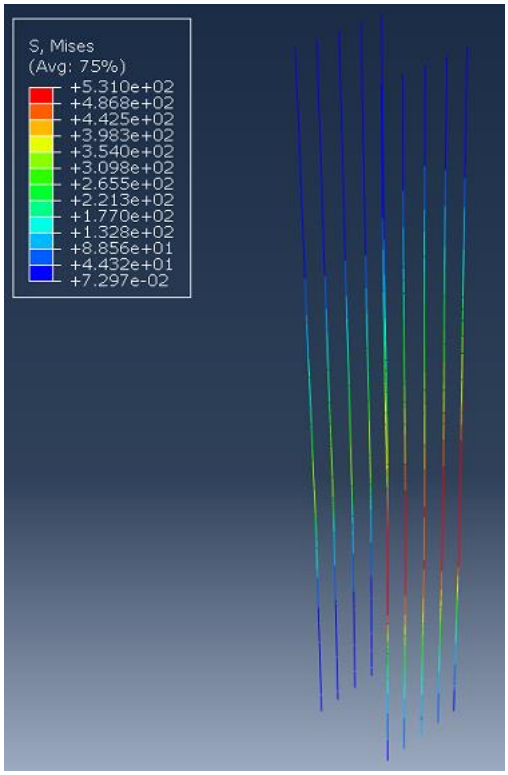

Figure 5.6: Principal stress for longitudinal steel reinforcement (CFRP strengthened)

5.3.4. Strain in CFRP

The effective strains on the CFRP strips due to combined shear action and concrete lateral dilatation are investigated. The effective strain on the CFRP wrappings is studied in the FE model and compared it with the experimental data. The ratio between CFRP experimental strain at positive peak drift (ε_f) and the ultimate strain in the CFRP (ε_{fu}) is recorded and the maximum value of this ratio of strain in experimental data is found to be at a drift of 4.8% on the side B and on the third strip. It was found to be around 30 %. Table 5.1 provides the strain in the CFRP calculated using the probe values (figure 5.7) for the relative displacement in each strip and on each side at a drift of 4.8 %. And it shows that the third strip have a ratio of $\varepsilon_f / \varepsilon_{fu,}$ of around 28.77 %. But the maximum is not showing in third strip in the numerical analysis. The maximum value of this ratio is happening in side D and for the second strip. The notable element here is that the even though the strain data doesn't completely coincide with the experimental data, the maximum strain happens in side B and D where the longitudinal reinforcement is absent.

Table 5.1: CFRP strain data

Side	A		B		C		D	
Strips	ε_f %	$\varepsilon_f/\varepsilon_{fu}$ %	ε_f %	$\varepsilon_f/\varepsilon_{fu}$ %	ε_f %	$\varepsilon_f/\varepsilon_{fu}$ %	ε_f %	$\varepsilon_f/\varepsilon_{fu}$ %
I	1.20E-02	0.63	1.80E-01	9.47	4.90E-01	25.79	5.57E-02	2.93
II	5.73E-01	30.17	8.43E-01	44.38	6.57E-01	34.56	1.04	54.91
III	5.40E-01	28.42	5.47E-01	28.77	2.63E-01	13.86	5.47E-01	28.77
IV	8.17E-02	4.29	1.77E-02	0.93	9.67E-03	0.51	1.77E-02	0.93

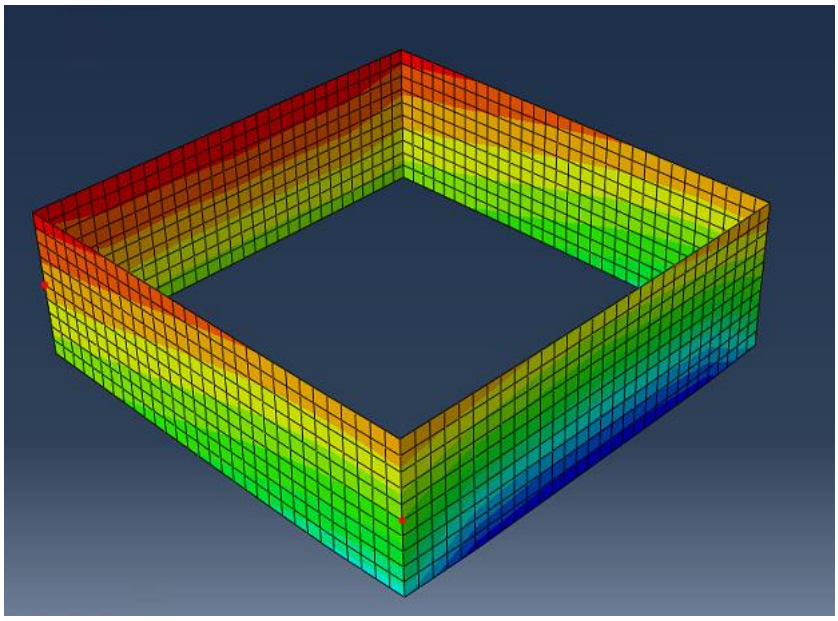

Figure 5.7: CFRP effective strain by probe values

Based on the provided data, it is evident that the carbon fibre reinforced polymer (CFRP) did not reach its ultimate strain of 1.9%. This observation aligns with the experimental strain analysis, where no CFRP strip reached its ultimate strain value. Although the experimental results showed local rupture of the CFRP, the numerical modelling study did not incorporate any failure criteria. Therefore, the analysis of CFRP failure is beyond the scope of this study.

5.4. Comparative Study of As-built Specimen and CFRP strengthened Specimen

The numerical and experimental study indicates a clear increase in capacity of the column when strengthened with CFRP. Figure 5.8 shows a comparison of experimental and numerical model of both

the as-built and CFRP strengthened specimen, where isotropic material for CFRP is considered for the numerical model result of S4.

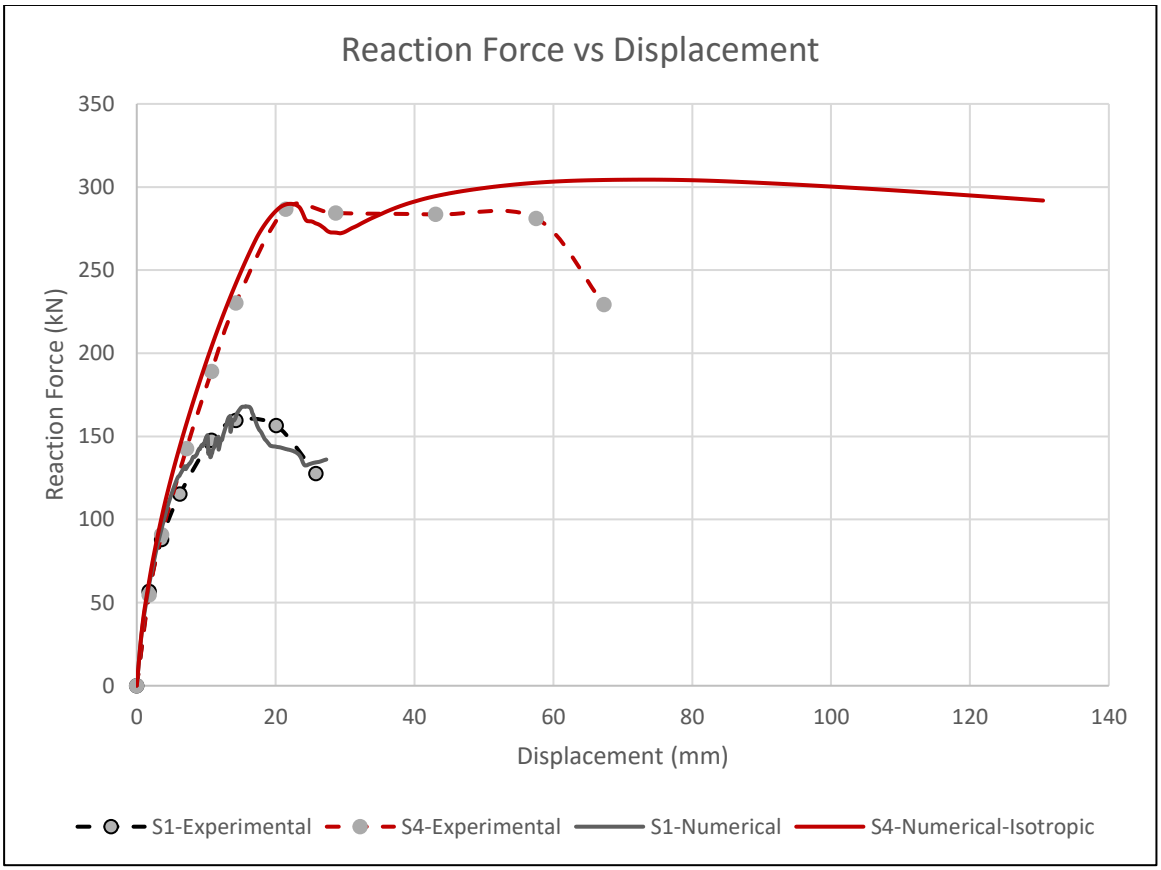

Figure 5.8: Comparative study of load-displacement curve for S1 and S4

Table 5.2: Load -displacement curve data comparison of S1 and S4

Specimen		Peak force (kN)	Displacement at peak force (mm)	Percentage deviation in peak force (%)	Percentage deviation in displacement (%)
S1	Experimental	159	14.29	5.4	8.9
	Numerical	168.15	15.69		
S4	Experimental	286.66	21.46	1.1	2.4
	Numerical	289.88	21.98		

Table 5.2 shows the comparison of peak force and the displacement corresponding to the peak force of the as-built and CFRP strengthened specimen. The deviation of numerical results from the experimental outcome showed to be less than 10 %. While comparing the numerical models of S1 and S4 the increase

in capacity is around 72.39 %. Whereas in the case of the experimental result, the capacity was increased by around 80 % which is comparable to the numerical model.

THIS PAGE WAS INTENTIONALLY LEFT BLANK

6. CONCLUSIONS AND FUTURE SCOPE

The main objectives of this study were to develop a numerical model using ABAQUS software to simulate the behaviour of reinforced concrete (RC) columns under quasi-static monotonic loading, and to investigate the effect of carbon fibre reinforced polymer (CFRP) strengthening on the column's performance. The study aimed to validate the numerical model by comparing its results with experimental data obtained from previous research conducted by D. Zoppo et al. [5] .

To achieve these objectives, a finite element (FE) model was created using ABAQUS software, incorporating the concrete damage plasticity model. Initially, the analysis focused on the as-built specimen, simulating its behaviour under loading conditions. Subsequently, the CFRP-strengthened specimen was introduced, and its performance was analysed using the numerical model.

The results of the numerical analysis revealed a significant increase in the capacity of the RC columns after CFRP strengthening, which was consistent with real-life scenarios. A model calibration was required in the case of the CFRP-strengthened specimen to match the experimental results accurately. It was observed that the as-built specimen model exhibited better agreement with the experimental load-displacement curve compared to the CFRP-strengthened specimen model.

The materials modelling aspect of the study required more detailed analysis and investigation to specify the outcomes accurately. This suggests that further refinement and calibration of the CFRP material models would be beneficial in achieving better alignment between numerical predictions and experimental results.

6.1. Conclusive remarks

The proposed FE model was generated and analysed and was validated based on the experimental behaviour. The major outcome of the study can be comprised of following:

1. The concrete damage plasticity model was used to model the RC columns.

2. Truss elements were suited to represent the deformed steel reinforcement and this assumption of no slip condition between the reinforcement and the concrete proved to be comparable with the real-life analysis.
3. Conventional shell elements showed promising results for modelling the CFRP wrappings.
4. The comparison of the load-displacement curves obtained from the finite element (FE) model indicated a significant improvement in the capacity of the CFRP-strengthened specimen. Specifically, the results showed a promising increase in capacity of approximately 72% when compared to the as-built specimen.
5. The envelope curve of the experimental hysteresis curve and the monotonic load displacement curve obtained for the numerical study showed a reasonable comparison with a variation less than 10 % from the experimental.
6. The CFRP strengthened specimen was found to be showing better comparison with the numerical model with an increase in dilation angle.
7. The capacity of steel in numerical analysis showed that the full capacity of steel was achieved in the case of CFRP strengthened specimen before reaching the peak as opposed to the as-built model, which indicates a ductile failure rather than a brittle one.
8. The CFRP strain in numerical analysis showed that no strips reached its ultimate value which was in agreement with the experimental observation.

6.2. Future Scope and Recommendation

As every study will provide a new stepping stone for the next stage, this study also proved that there are areas where things can be improved. The study was conducted as a first step towards the development of reliable and accurate design equation for FRP strengthening of columns under gravity and horizontal loads, which is a crucial goal in multi-risk assessment of existing structures. The model developed here can be used for designing and modelling an RC column with CFRP strengthening. This can be improved by following:

1. While inputting the material properties in the FE model, it is better to input them based on accurate experimental analyses. For example, conducting several tension and compression tests on the concrete cylinder the exact stress-strain behaviour can be captured and this will help to model the non-linear part as well as designing the damage parameters in ABAQUS.

2. Accurate designing of the damage parameter helps to capture the material degradation of concrete. This has to be determined experimentally which then can be used as a data input to the concrete damage plasticity.
3. The influence of dilation angle on the confinement is another important area of study. To find the exact influence of dilation angle with the CFRP wrapping can help to achieve results comparable to the experimental outcomes.
4. While analysing the CFRP, in this model only elastic limit has been taken into consideration. It is better to model the damage mechanism associated with CFRP to reproduce the exact result in the experiment. For that material characterisation of the laminate will give the input parameters for modelling the damage of composite.
5. Considering CFRP as a laminate rather than isotropic can also influence the results and for convergence mesh refinement along with explicit analysis can be done.

THIS PAGE WAS INTENTIONALLY LEFT BLANK

REFERENCES

[1] "Rehabilitation and strengthening techniques for reinforced concrete columns: review", doi: 10.1088/1742-6596/1895/1/012049.

[2] G. , C. F. , C. L. , F. M. F. , & P. M. Campione, " Assessment of the load carrying capacity of reinforced concrete columns strengthened by steel cages Specificità nella valutazione della capacità portante di colonne in calcestruzzo armato rinforzate con incamiciatura in acciaio," in *In Proceedings of Italian Concrete Days 2018. di Prisco, Marco, Menegotto, Marco.*, 2018.

[3] K. SH and K. FR, "Review on the Strengthening of Reinforced Concrete Columns by Reinforced Concrete Jacketing," *Saudi Journal of Civil Engineering*, vol. 04, no. 01, pp. 10–20, Jan. 2020, doi: 10.36348/sjce.2020.v04i01.002.

[4] O. , I. D. , & H. R. Stanila, "Timber Elements: Traditional and Modern Strengthening Techniques," *uletinul Institutului Politehnic din Iasi. Sectia Constructii, Arhitectura, 56(3), 75.* 2010.

[5] M. Del Zoppo, M. Di Ludovico, A. Balsamo, A. Prota, and G. Manfredi, "FRP for seismic strengthening of shear controlled RC columns: Experience from earthquakes and experimental analysis," *Compos B Eng*, vol. 129, pp. 47–57, Nov. 2017, doi: 10.1016/j.compositesb.2017.07.028.

[6] A. Kargaran and A. Kheyroddin, "Experimental and numerical investigation of seismic retrofitting of RC square short columns using FRP composites," *European Journal of Environmental and Civil Engineering*, vol. 26, no. 10, pp. 4619–4642, Jul. 2022, doi: 10.1080/19648189.2020.1858171.

[7] S. M. Hosseini and D. Mostofinejad, "Seismic Performance of RC Short Columns Retrofitted with a Novel System in Shear and Flexure Using CFRP Composites," *Journal of Composites for Construction*, vol. 25, no. 5, Oct. 2021, doi: 10.1061/(ASCE)CC.1943-5614.0001148.

[8] M. Del Zoppo, M. Di Ludovico, A. Balsamo, and A. Prota, "Comparative Analysis of Existing RC Columns Jacketed with CFRP or FRCC," *Polymers (Basel)*, vol. 10, no. 4, p. 361, Mar. 2018, doi: 10.3390/polym10040361.

[9] J.-H. Song, E.-T. Lee, and H.-C. Eun, "Shear Strength of Reinforced Concrete Columns Retrofitted by Glass Fiber Reinforced Polyurea," *Civil Engineering Journal*, vol. 6, no. 10, pp. 1852–1863, Oct. 2020, doi: 10.28991/cej-2020-03091587.

[10] K. Gajdosova and J. Bilcik, "Full-Scale Testing of CFRP-Strengthened Slender Reinforced Concrete Columns," *Journal of Composites for Construction*, vol. 17, no. 2, pp. 239–248, Apr. 2013, doi: 10.1061/(ASCE)CC.1943-5614.0000329.

[11] Y. Li, S. Yin, J. Dai, and M. Liu, "Numerical investigation on the influences of different factors on the seismic performance of TRC-strengthened RC columns," *Journal of Building Engineering*, vol. 30, p. 101245, Jul. 2020, doi: 10.1016/j.jobe.2020.101245.

[12] F. Danesh, E. Esmaeeli, and M. F. Alam, "Shear Strengthening of 3D RC Beam-Column Connection Using GFRP: FEM Study," *Asian Journal of Applied Sciences*, vol. 1, no. 3, pp. 217–227, Jun. 2008, doi: 10.3923/ajaps.2008.217.227.

[13] M. Altaee, M. Kadhim, S. Altayee, and A. Adheem, "Employment of damage plasticity constitutive model for concrete members subjected to high strain-rate," in *Proceedings of the Proceedings of the 1st International Multi-Disciplinary Conference Theme: Sustainable Development and Smart Planning, IMDC-SDSP 2020, Cyperspace, 28-30 June 2020*, EAI, 2020. doi: 10.4108/eai.28-6-2020.2298164.

[14] J. Lee and G. L. Fenves, "Plastic-Damage Model for Cyclic Loading of Concrete Structures," *J Eng Mech*, vol. 124, no. 8, pp. 892–900, Aug. 1998, doi: 10.1061/(ASCE)0733-9399(1998)124:8(892).

[15] J. Lubliner, J. Oliver, S. Oller, and E. Oñate, "A plastic-damage model for concrete," *Int J Solids Struct*, vol. 25, no. 3, pp. 299–326, 1989, doi: 10.1016/0020-7683(89)90050-4.

[16] "Eurocode 2: Design of concrete structures-Part 1-1: General rules and rules for buildings," 2004.

[17] "abaqus documentation 6.9 - Google Scholar." https://scholar.google.com/scholar?hl=en&as_sdt=0%2C5&q=abaqus+documentation+6.9&btnG= (accessed May 30, 2023).

[18] S. K. John, Y. Nadir, and K. Girija, "Nonlinear finite element modelling of concrete columns confined with textile reinforced mortar," *IOP Conf Ser Earth Environ Sci*,

vol. 491, no. 1, p. 012022, Jun. 2020, doi: 10.1088/1755-1315/491/1/012022.

[19] A. Demir, H. Ozturk, K. Edip, M. Stojmanovska, and A. Bogdanovic, "EFFECT OF VISCOSITY PARAMETER ON THE NUMERICAL SIMULATION OF REINFORCED CONCRETE DEEP BEAM BEHAVIOR," *The Online Journal of Science and Technology*, vol. 8, no. 3, Jul. 2018.

[20] fib, *fib Model Code for Concrete Structures 2010*. Weinheim, Germany: Wiley-VCH Verlag GmbH & Co. KGaA, 2013. doi: 10.1002/9783433604090.

[21] M. Hafezolghorani, F. Hejazi, R. Vaghei, M. S. Bin Jaafar, and K. Karimzade, "Simplified Damage Plasticity Model for Concrete," *Structural Engineering International*, vol. 27, no. 1, pp. 68–78, Feb. 2017, doi: 10.2749/101686616X1081.

[22] "A General Shear Design Method," *ACI Struct J*, vol. 93, no. 1, 1996, doi: 10.14359/9838.

[23] S.-J. Mei, Y.-L. Bai, J.-G. Dai, and Q. Han, "Seismic behaviour of shear critical square RC columns strengthened by large rupture strain FRP," *Eng Struct*, vol. 280, p. 115679, Apr. 2023, doi: 10.1016/j.engstruct.2023.115679.

[24] Q. Sun *et al.*, "Failure criteria of unidirectional carbon fiber reinforced polymer composites informed by a computational micromechanics model," *Compos Sci Technol*, vol. 172, pp. 81–95, Mar. 2019, doi: 10.1016/j.compscitech.2019.01.012.

[25] A. K. Yadav and A. Poudel, "Study of Crack Pattern in RCC Beam Using ABAQUS," *Saudi Journal of Civil Engineering*, pp. 116–123, 2021.

[26] R. Bhartiya, D. R. Sahoo, and A. Verma, "Modified damaged plasticity and variable confinement modelling of rectangular CFT columns," *J Constr Steel Res*, vol. 176, p. 106426, Jan. 2021, doi: 10.1016/j.jcsr.2020.106426.